

Anatomy of Parity-Violating Trispectra in Galaxy Surveys

Yi-Ming Zhong



**w/ Yunjia Bao, Lian-Tao Wang and Zhong-Zhi Xianyu,
arXiv:2504.02931**

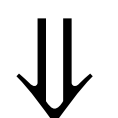
The 2025 Beijing Particle Physics and Cosmology Symposium, 26 September 2025

Outline

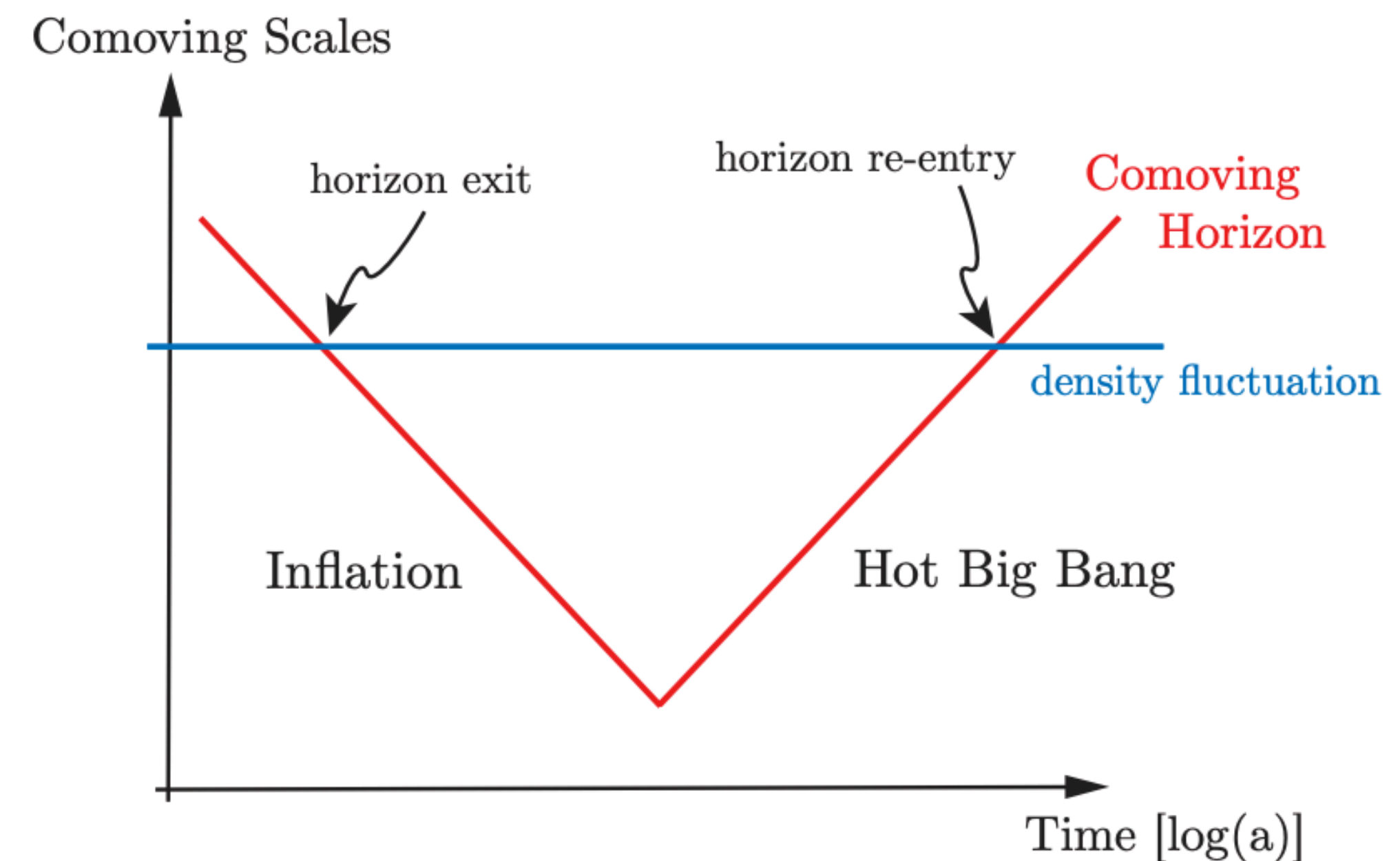
- Introduction
- Formalism
- Parity violating processes:
 - Toy models
 - Full models
- Results
- Summary

Inflation

- The leading paradigm to solve the flatness problem and the horizon problem.
- Quantum fluctuations got stretched and imprinted at superhorizon scales.



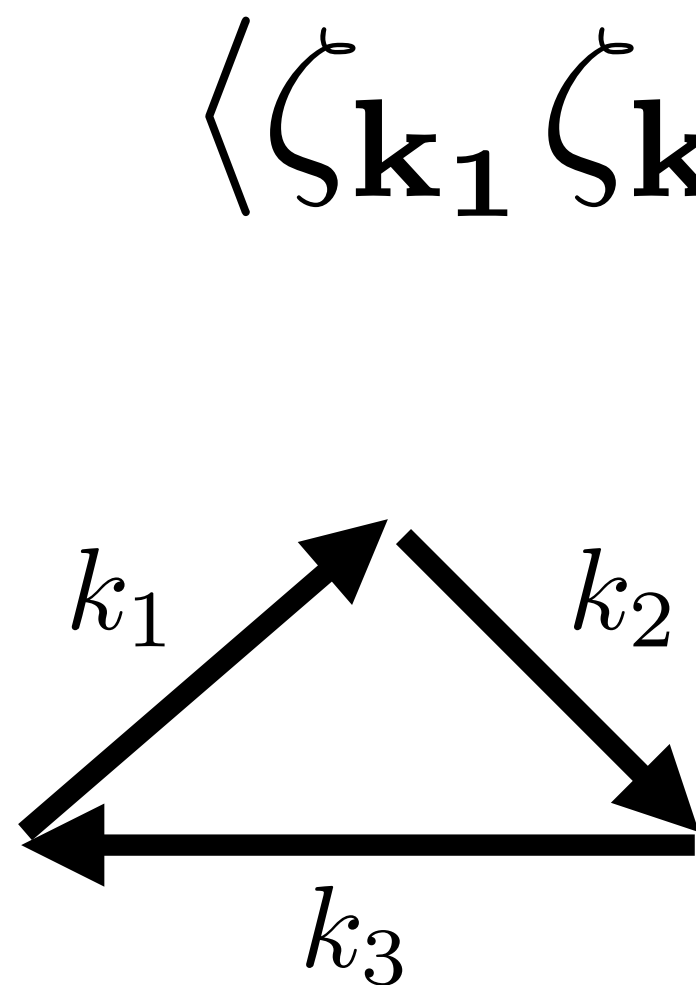
Explaining the origin of the inhomogeneity and anisotropy of our universe.

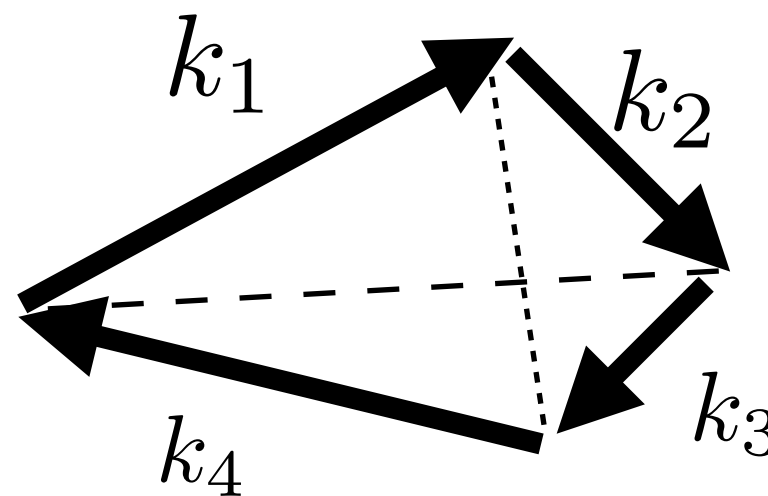


Baumann '12

Primordial non-Gaussianity (PNG)

- The simplest *single-field slow-roll* inflation predicts a **Gaussian** primordial spectra \Rightarrow nothing new in higher-pt correlators

$$\langle \zeta_{\mathbf{k}_1} \zeta_{\mathbf{k}_2} \zeta_{\mathbf{k}_3} \rangle' = 0$$




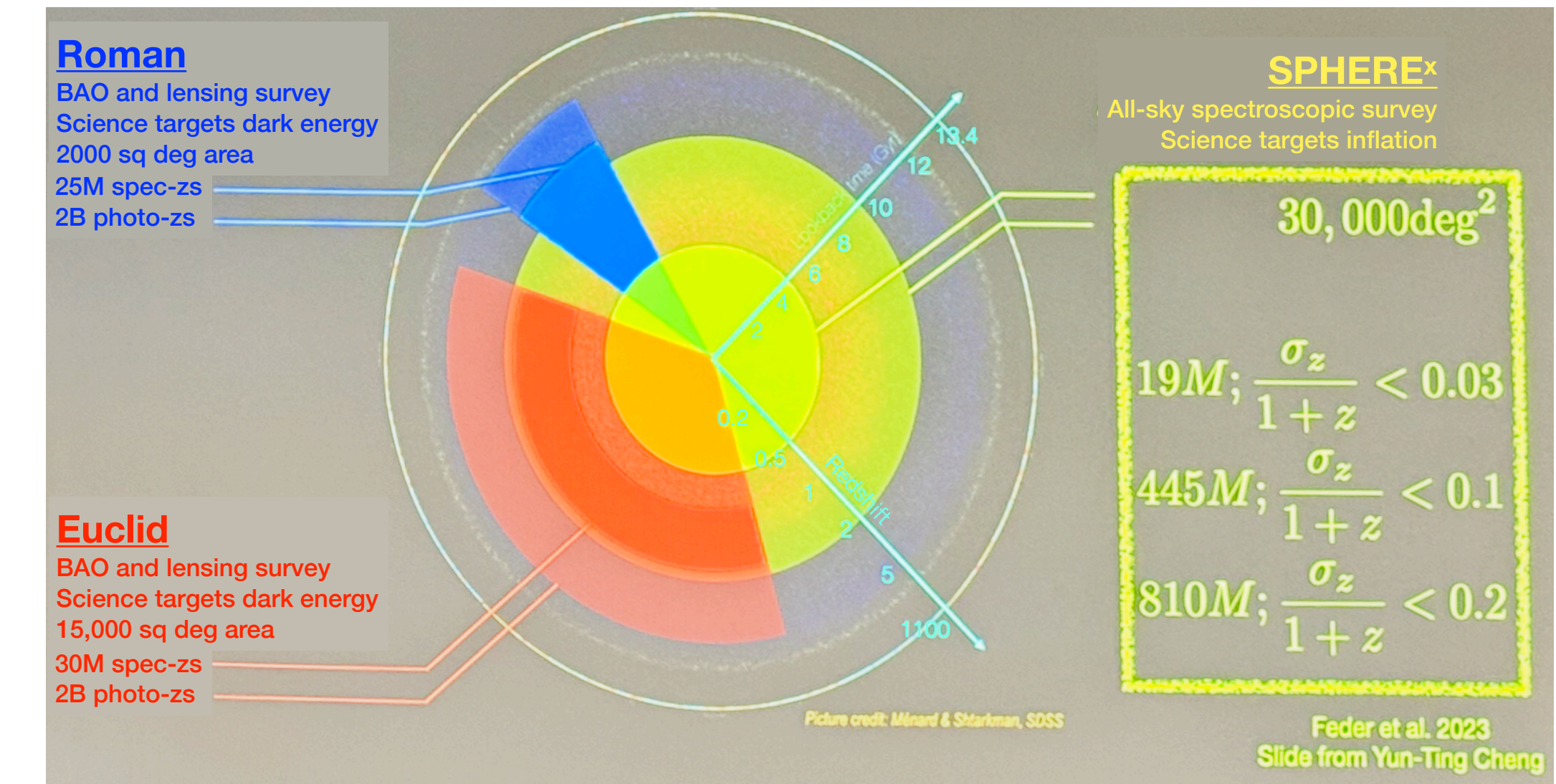
- Many inflation models predict non-trivial higher-pt correlators

$$\langle \zeta_{\mathbf{k}_1} \zeta_{\mathbf{k}_2} \zeta_{\mathbf{k}_3} \rangle' = ?$$

- break degeneracies of inflation models
- probe physics at very high energy scales

Searching for PNGs in galaxy surveys

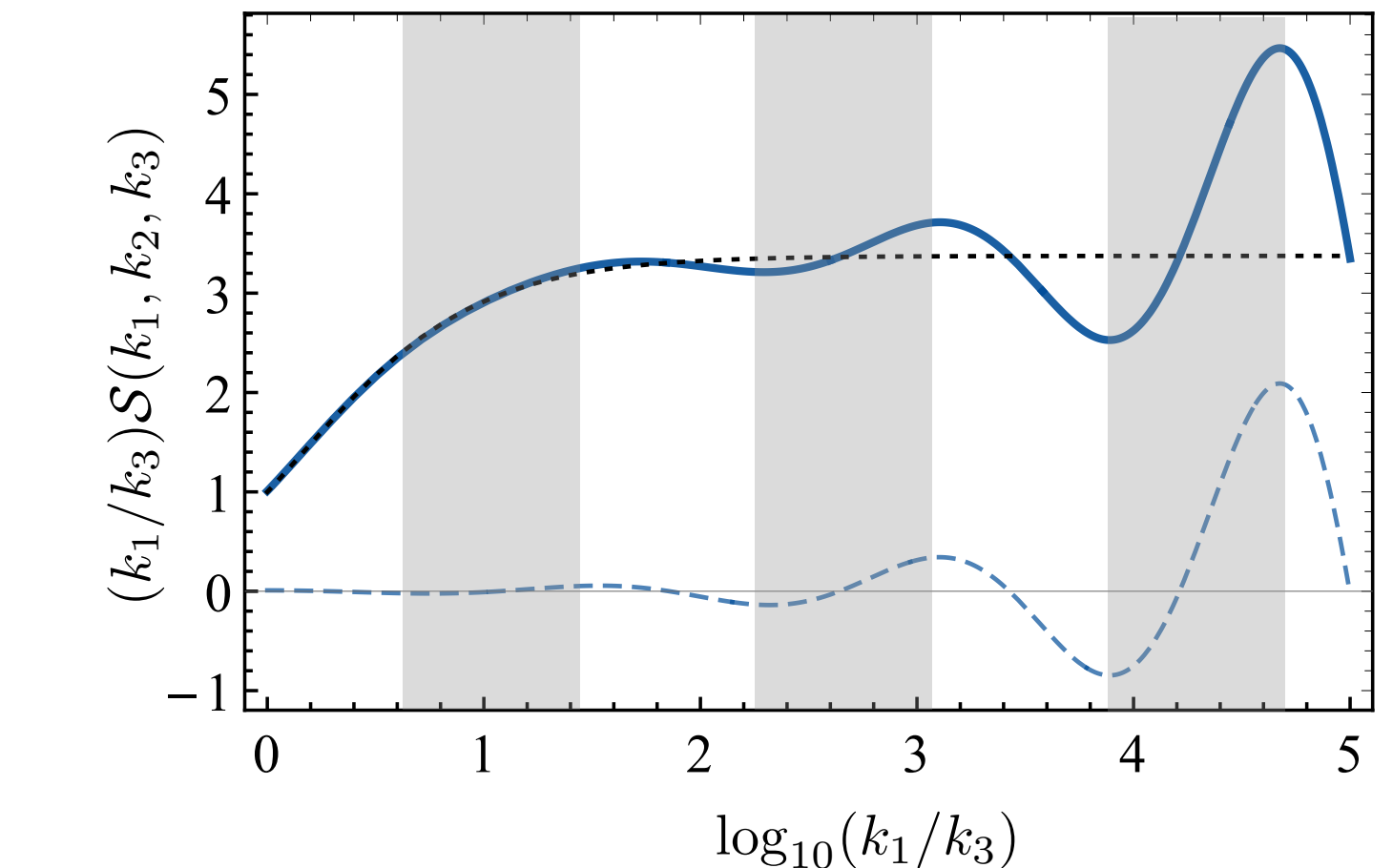
- PNGs can be searched in CMB / Large-Scale Structure surveys.
- 😊 There are abundant galaxy data from current and upcoming galaxy surveys.
- 😞 Observed NG = PNG + late-universe NG induced by gravity and baryonic physics.



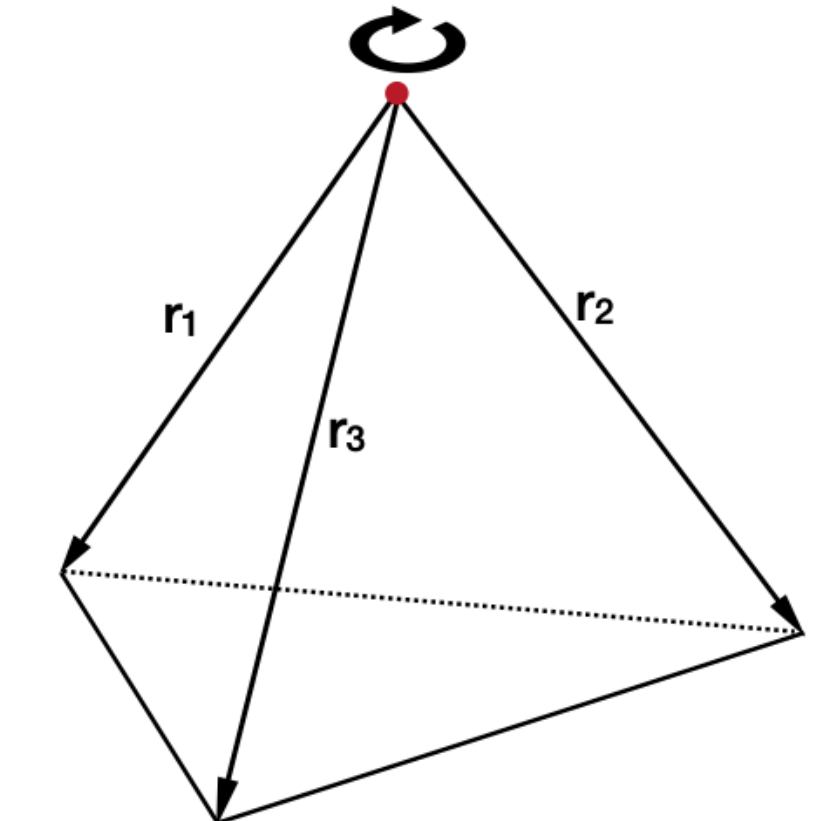
From Howard Hui's talk

What to do?

- A better understanding of late-time effects via dedicated modeling and simulations.
- Looking for targets that are robust against late-time effects.
 - **Cosmological collider signals.**
(Gravity & EM unlikely to induce the log oscillations.)
 - **Parity violation signals.**
(Gravity & EM should preserve parity.)

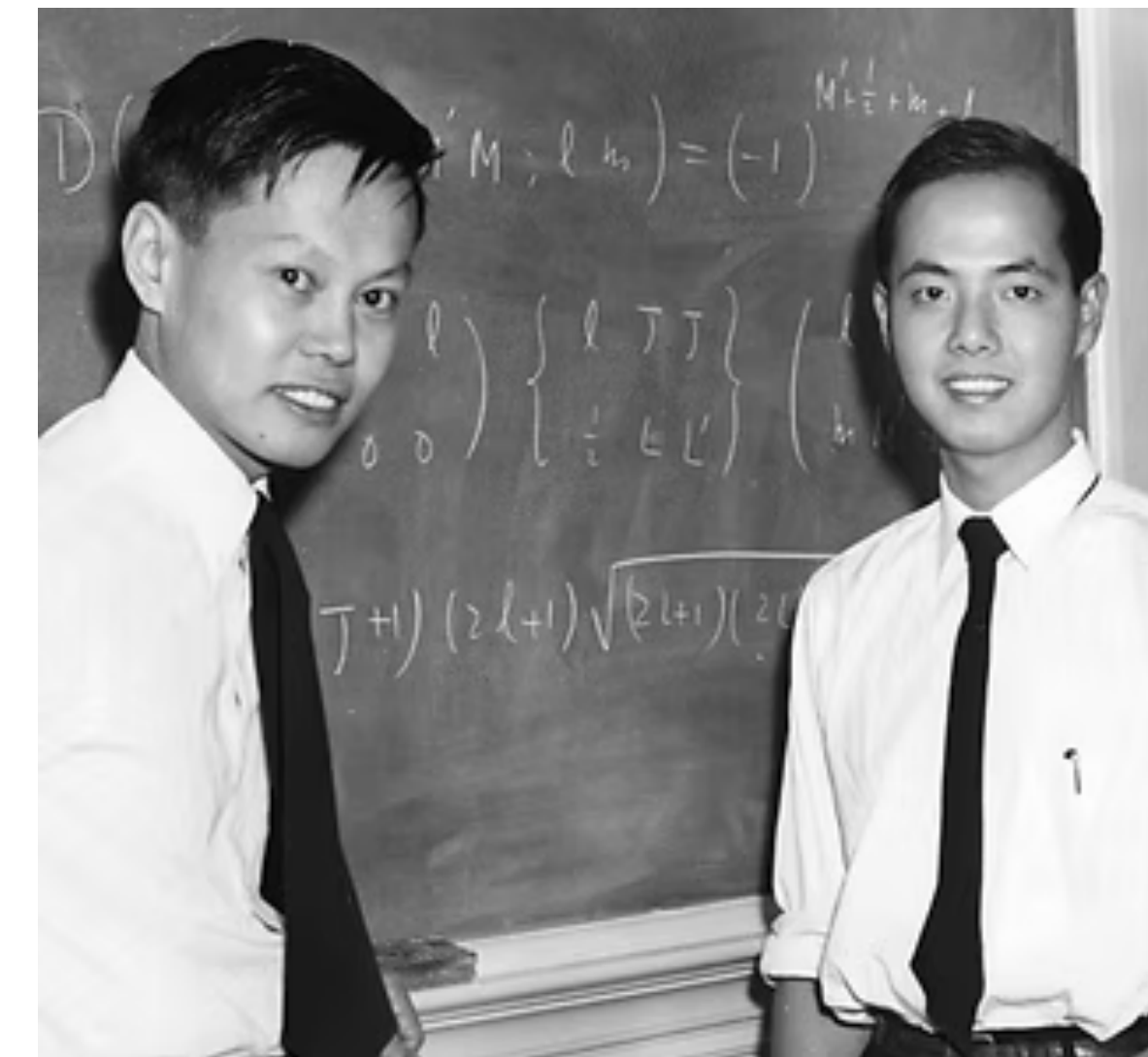


See Xianyu's talk



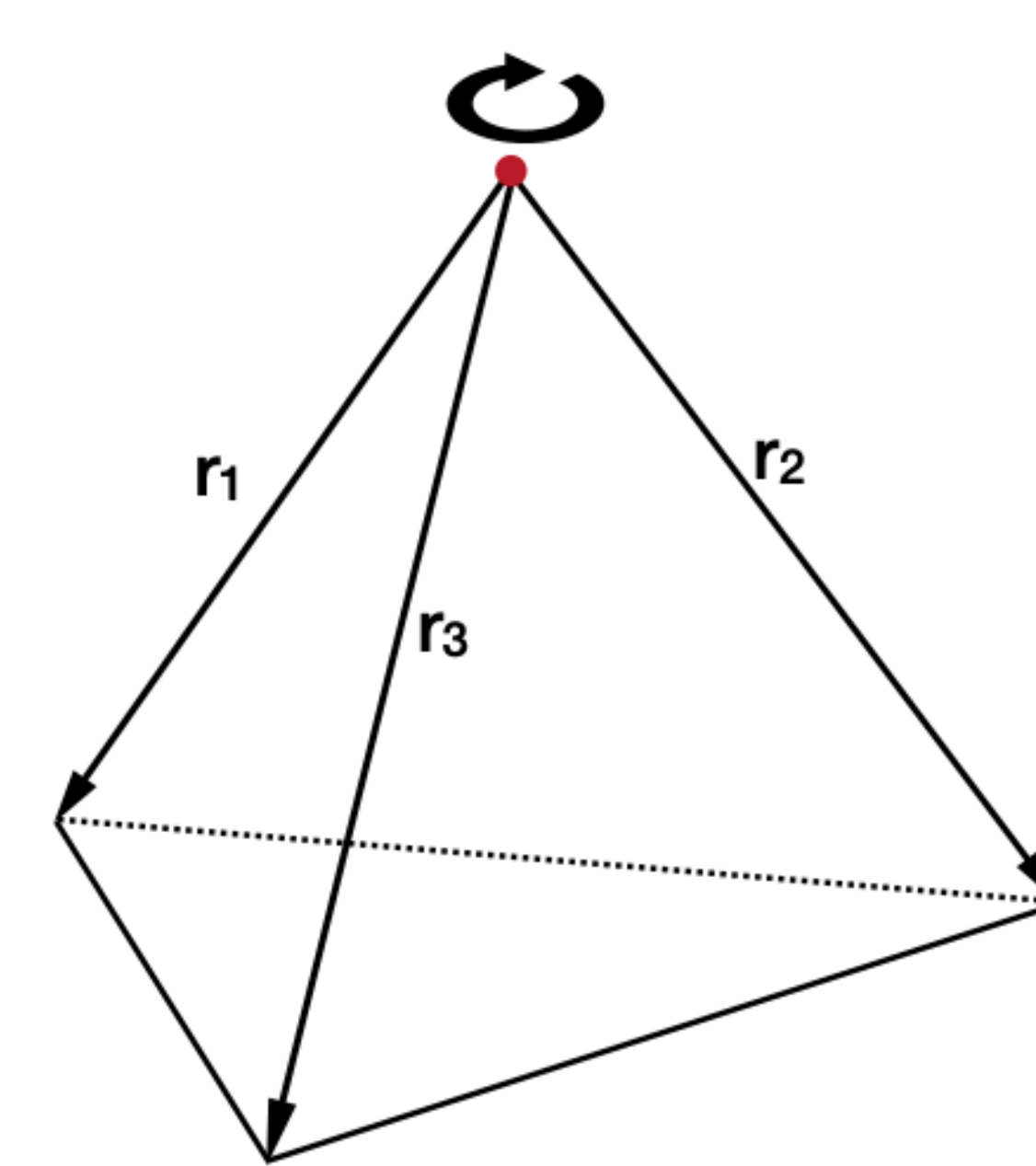
Parity-violation in large-scale structures

- Parity-violating processes are well-motivated and ubiquitous.
- They can happen during inflation and generate parity-violating PNGs.
- They will be preserved in the late time.

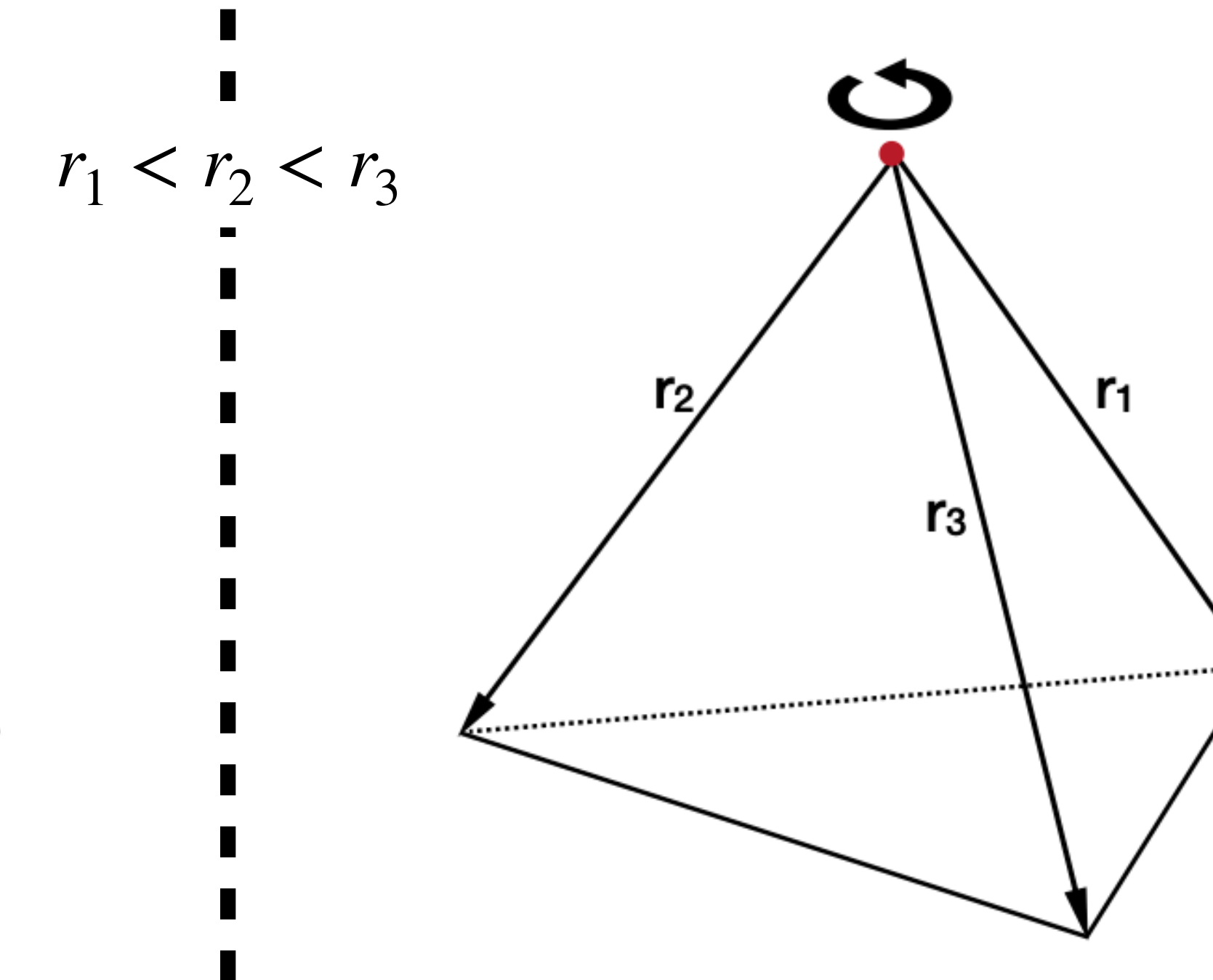


e.g., Anber & Sorbo '10, Barnaby+ '09, Liu+ '20 , Cabass+ '23, Stefanyszyn+ '24A, '24B, Fujita+ '24, Niu+ '23, Creque-Sarbinowski+ '23, Reinhard+ '24,.....

Parity-violations in four-point correlation function (4PCF)



Left-handed 4PCF



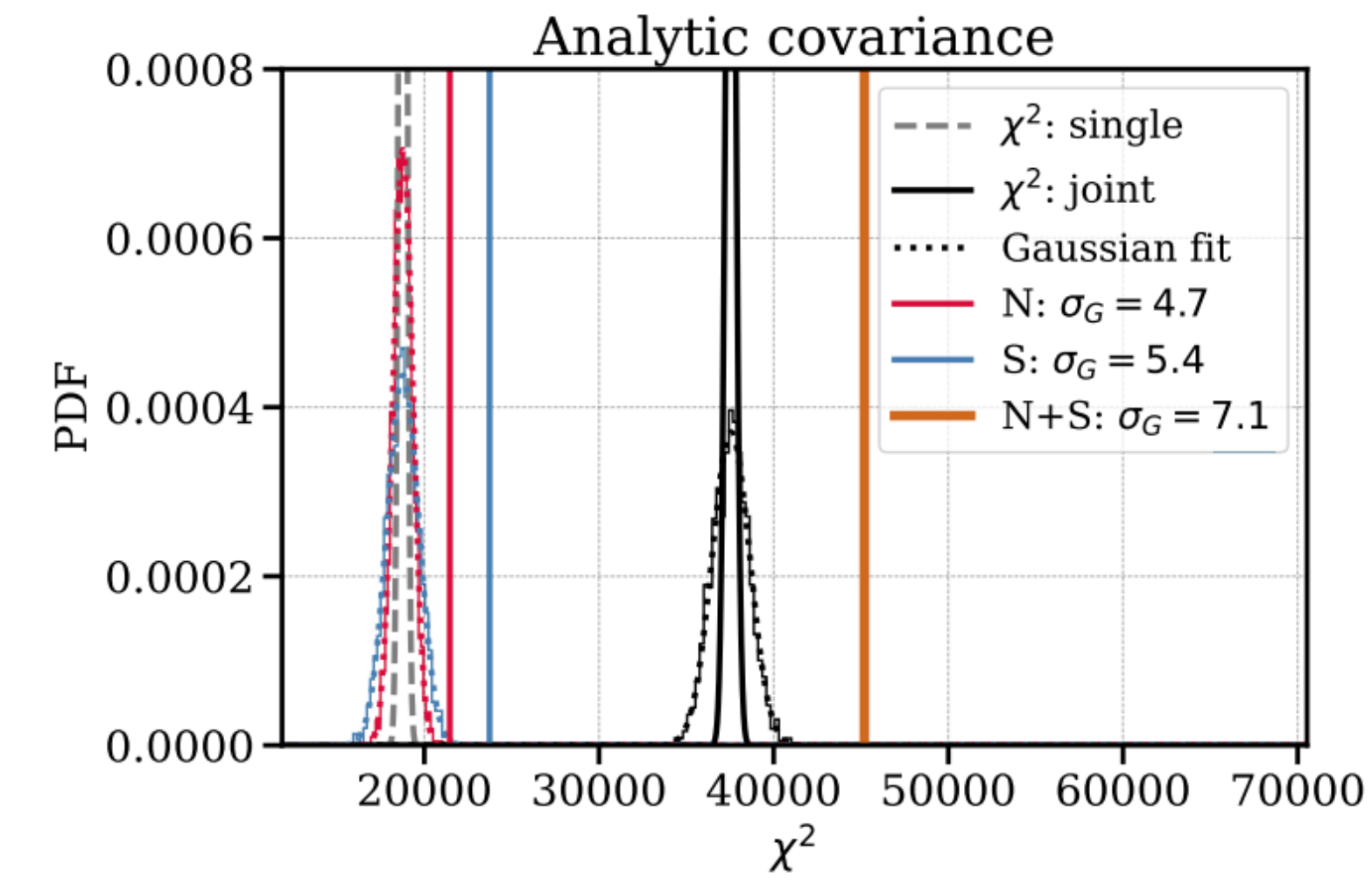
Right-handed 4PCF

Hou+ '22

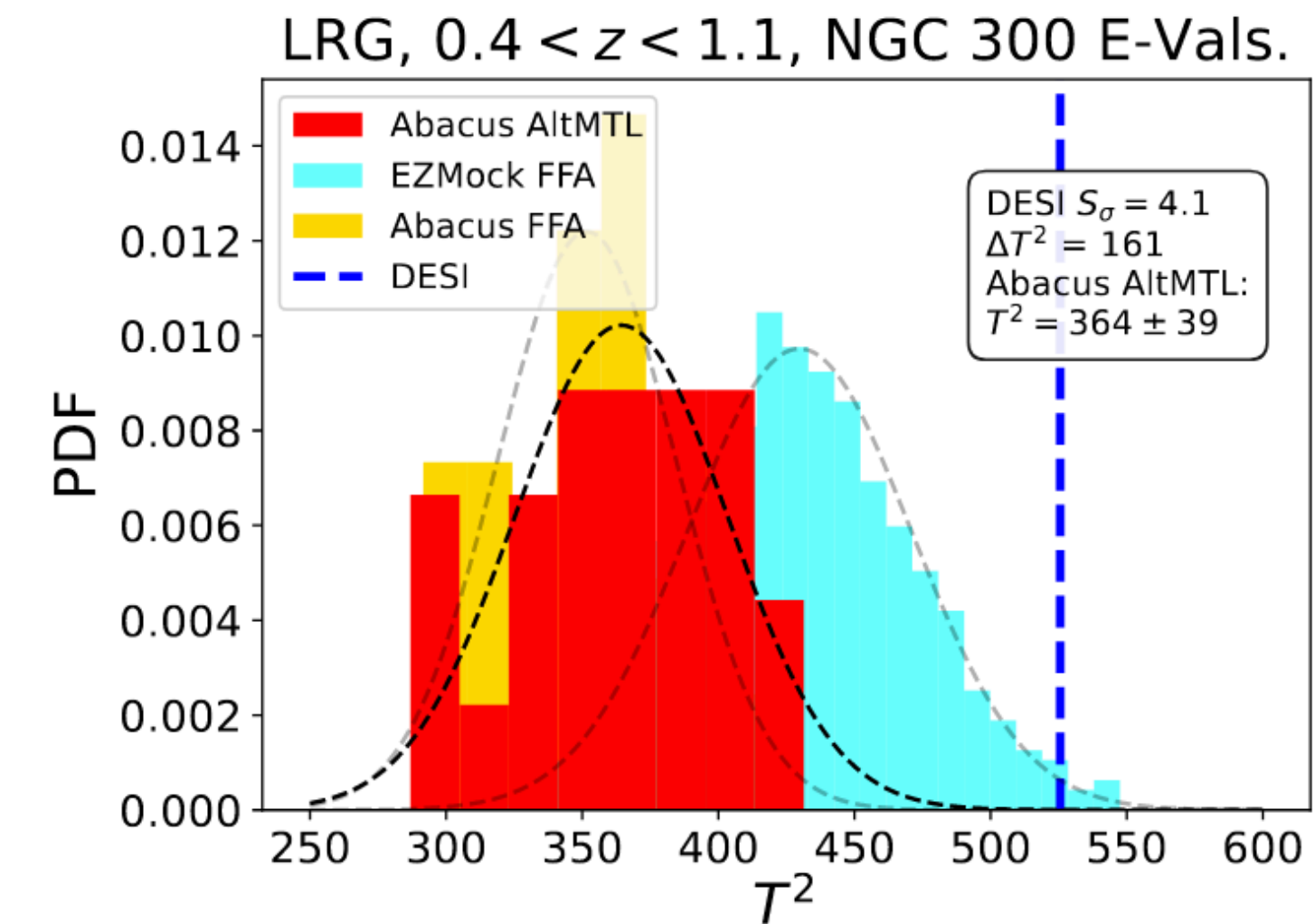
$$\text{Parity violation} = (\text{left-handed 4PCF}) - (\text{right-handed 4PCF})$$

Current status

- Philcox (2022) and Hou, Slepian & Cahn (2022) respectively detected the parity-violating 4PCF at $2\text{-}3\sigma$ and $4\text{-}7\sigma$ in BOSS data.
- Slepian et al. (2025) detected the parity-violating 4PCF at $4\text{-}10\sigma$ in DESI Y1 data.
- Pushbacks over the actual significance. See Krolewski et al. (2024), Philcox & Ereza (2024).



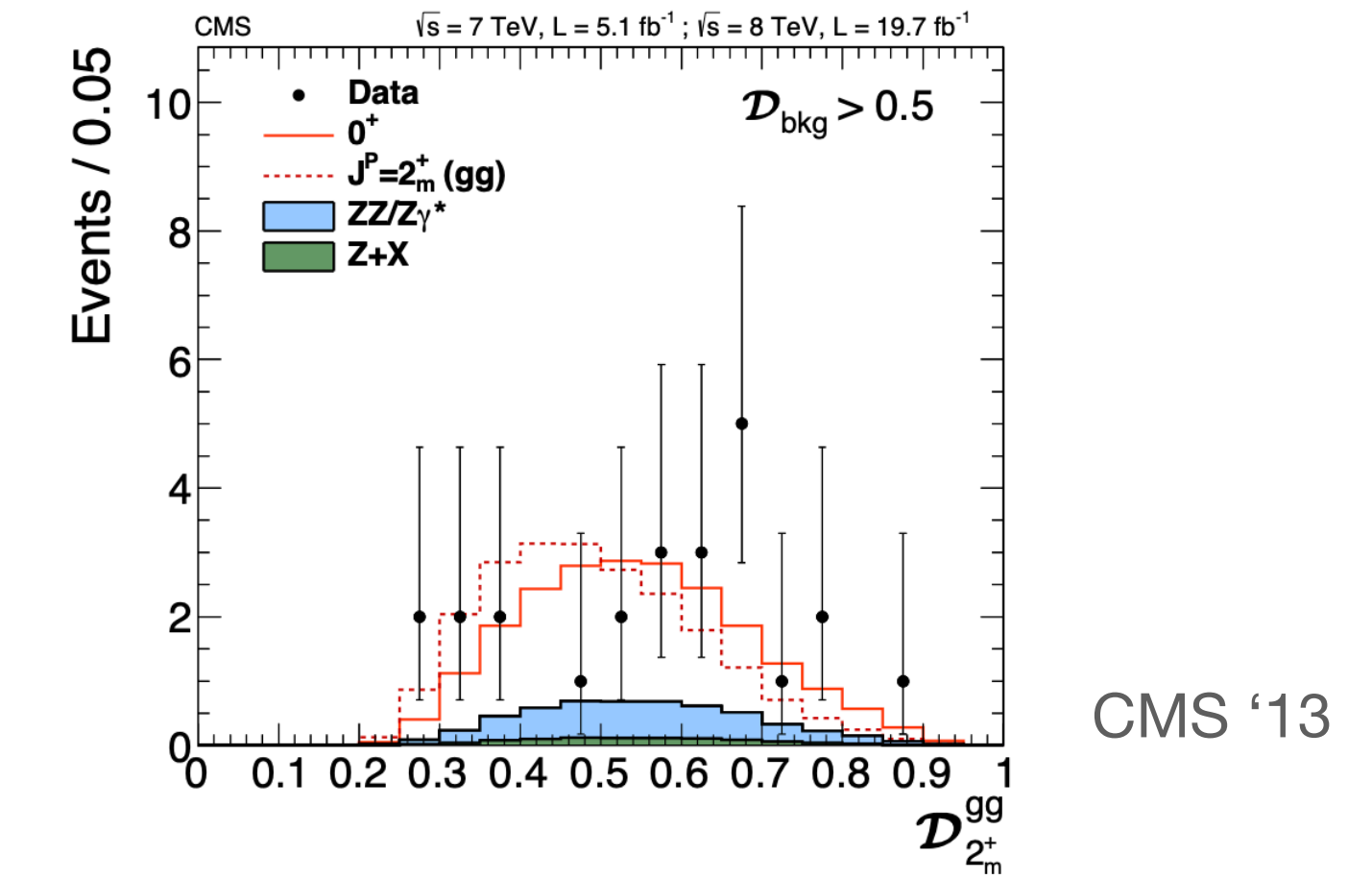
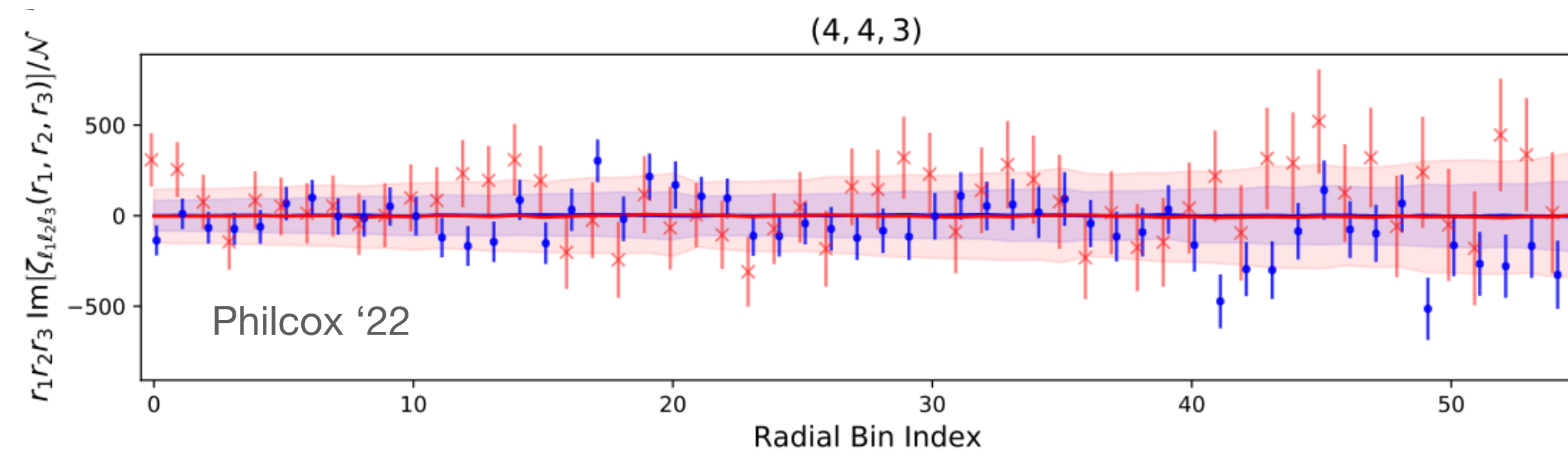
Hou+ '22

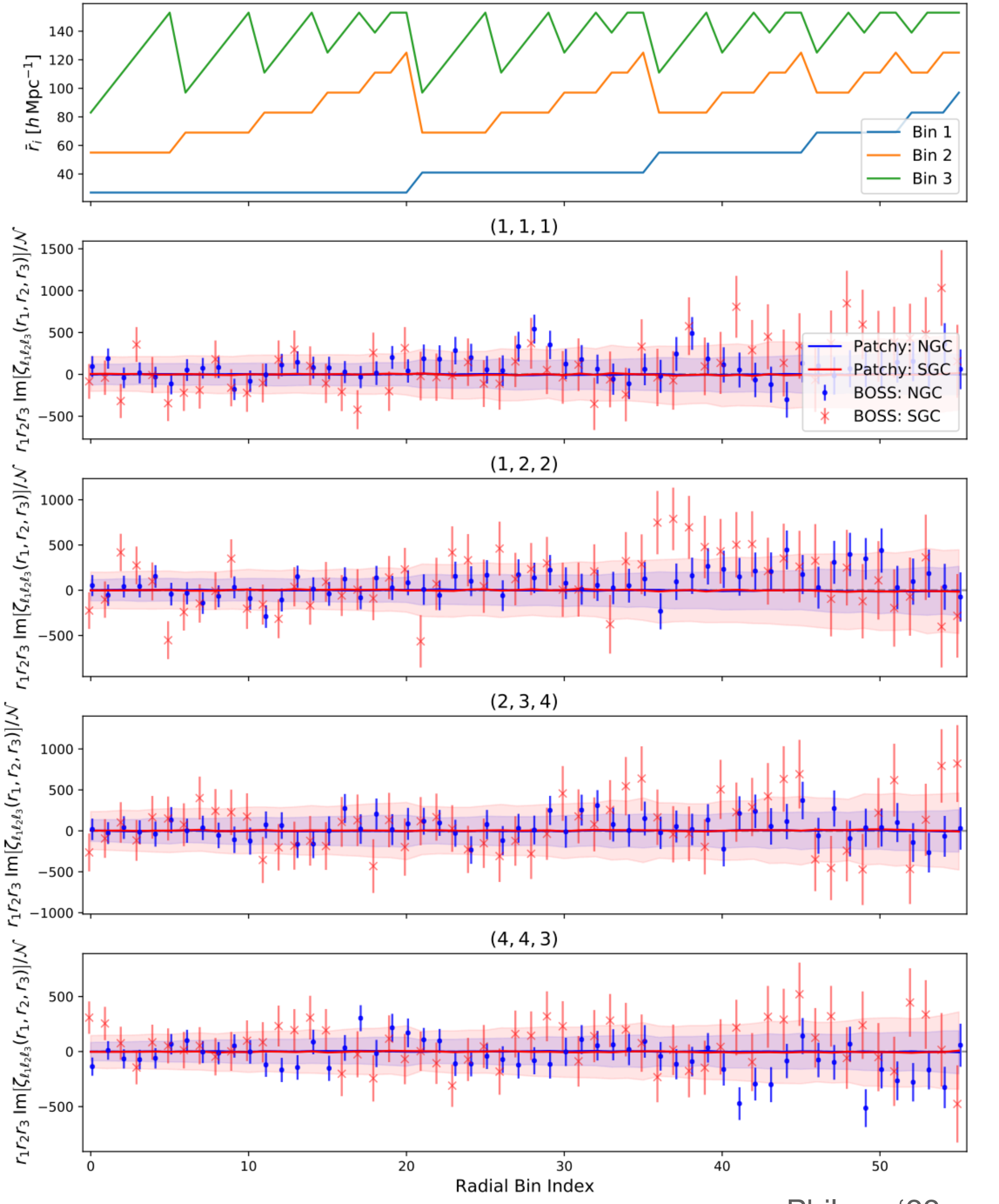


Slepian+ '25

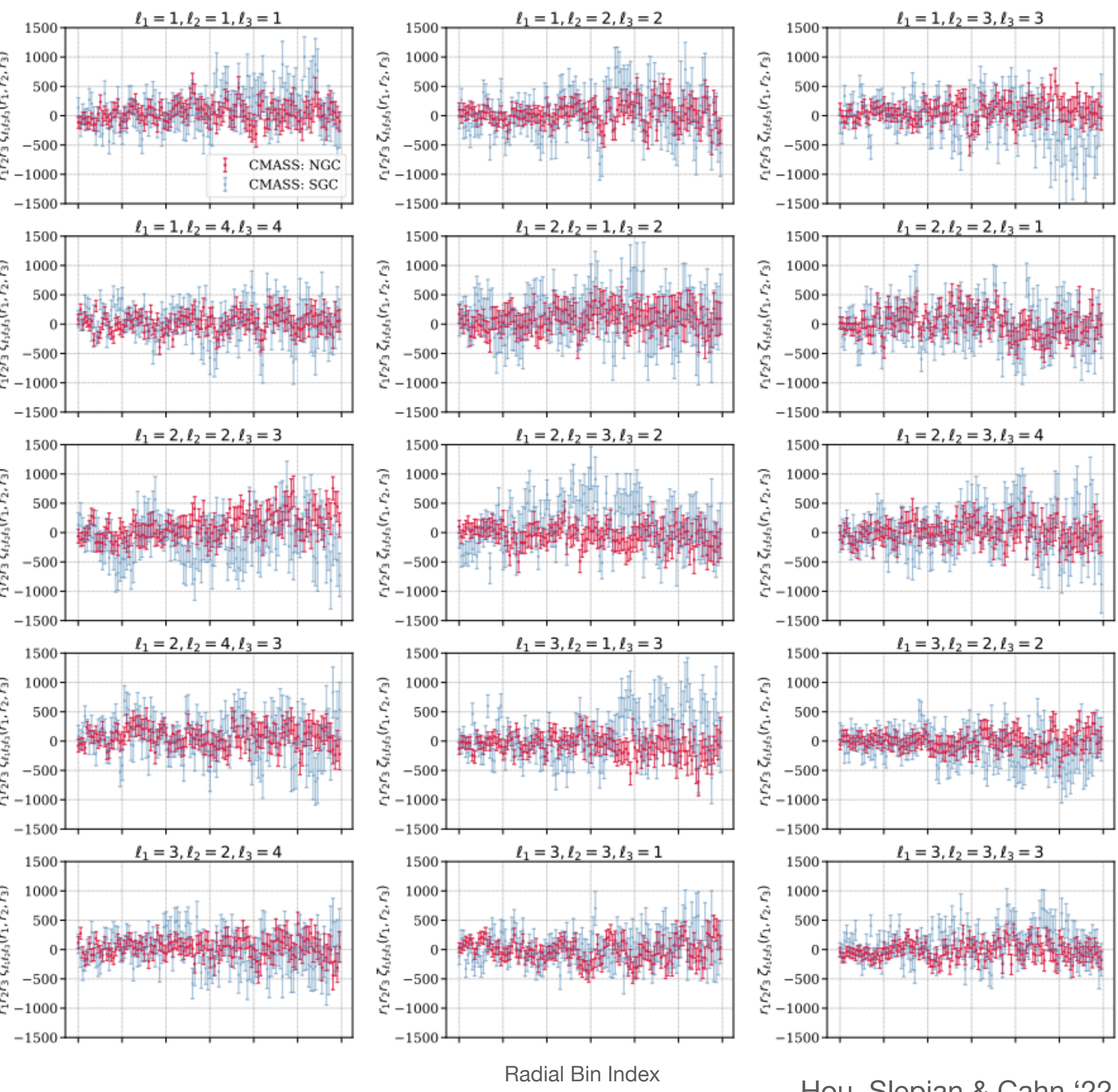
If it is true, what is the next?

- For cosmological colliders, we can learn mass/spin/interactions etc from the oscillation patterns.
- Can we learn something from the parity violating 4PCF?
- Philcox (2022) and Hou, Slepian & Cahn (2022) also give the signal distributions across **bins**. Those distributions can be used to differentiate various parity-violating models.





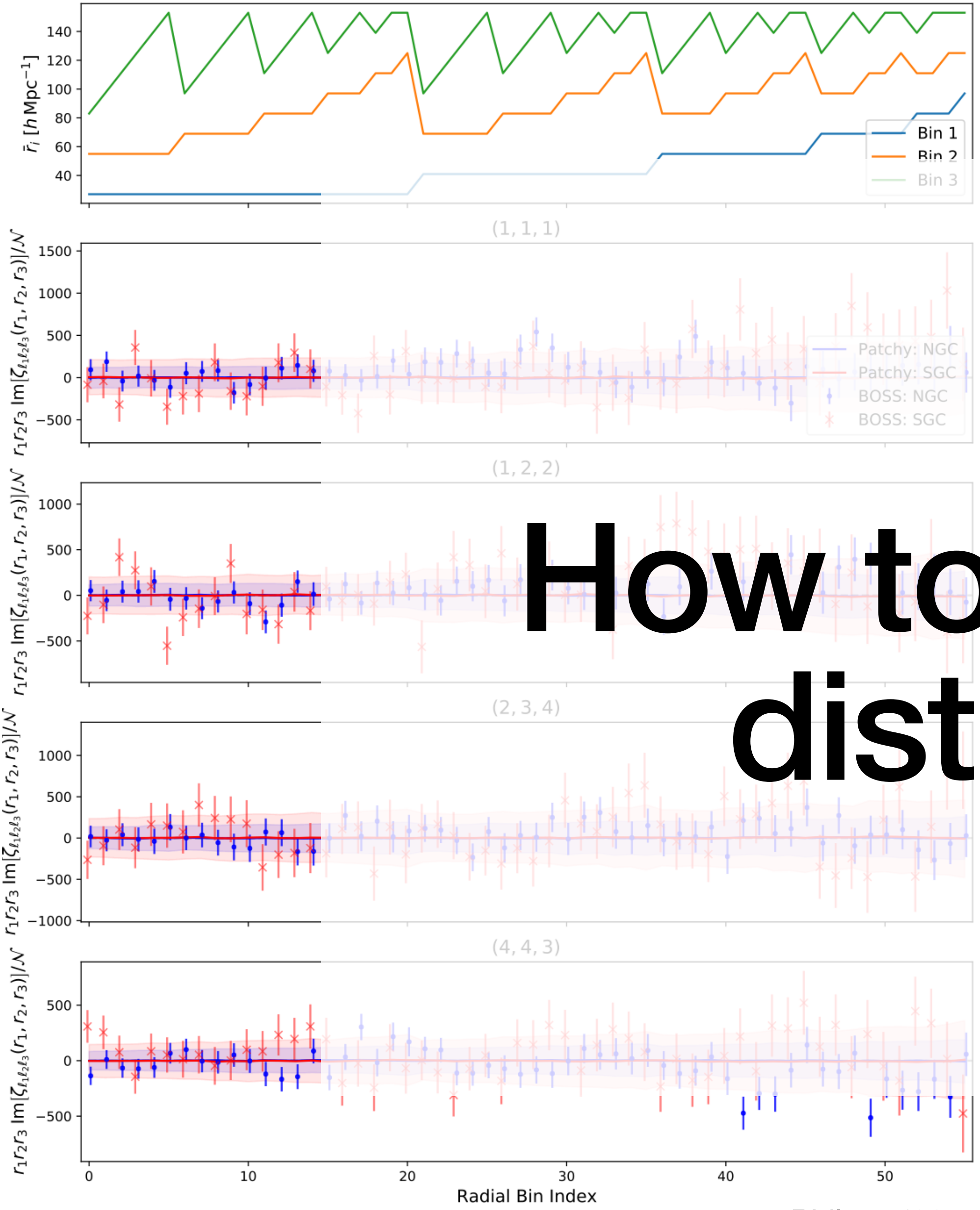
Philcox '22



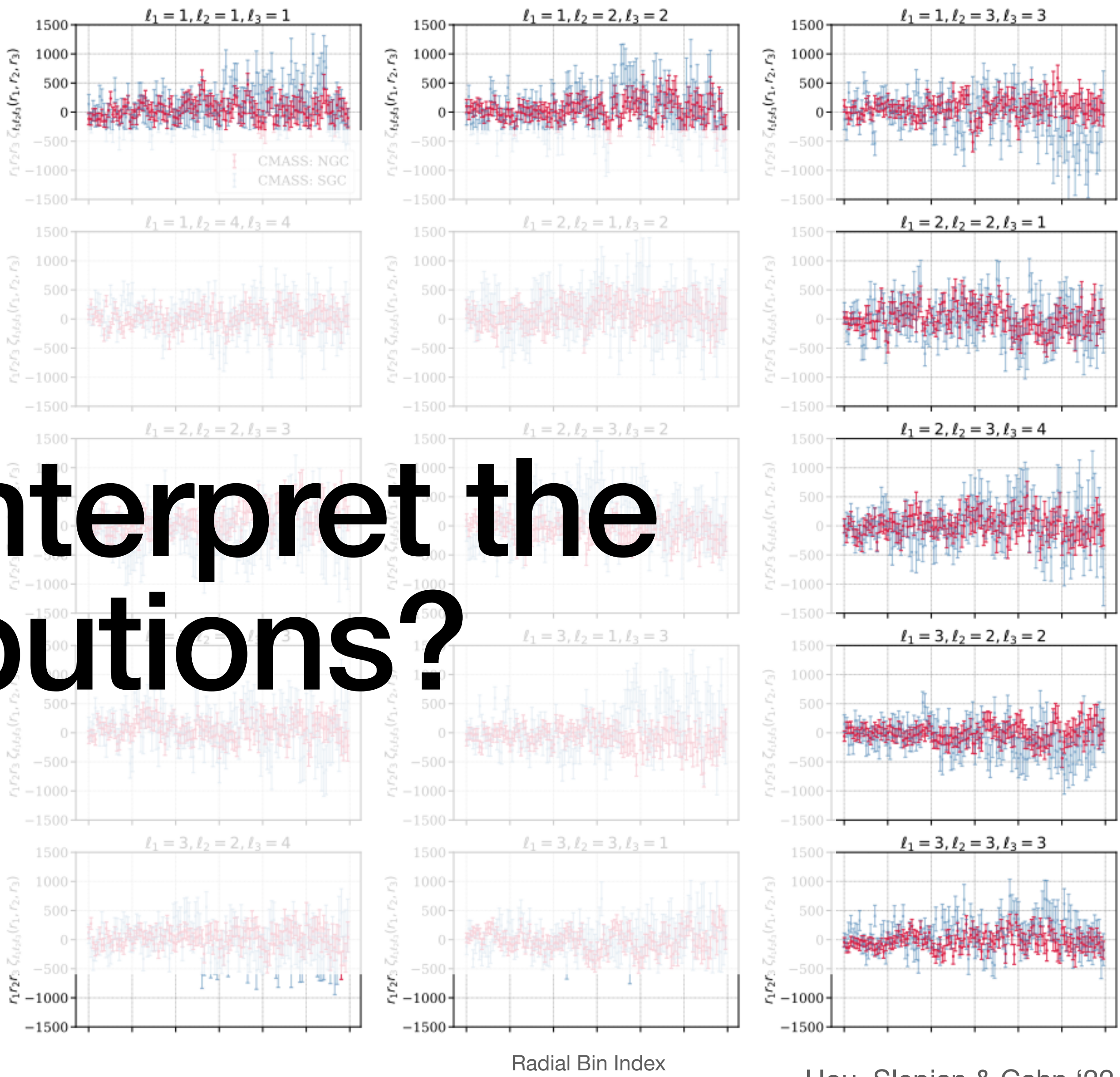
Radial Bin Index

Hou, Slepian & Cahn '22

How to interpret the distributions?



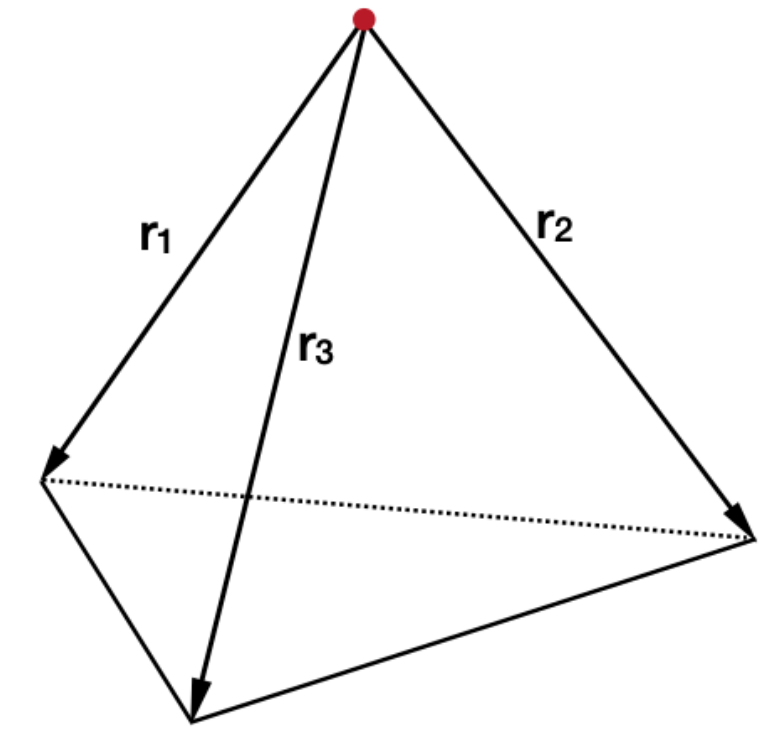
Philcox '22



Hou, Slepian & Cahn '22

Formalism

Galaxy overdensity 4PCF



$$\zeta_g^4(\mathbf{r}_1, \mathbf{r}_2, \mathbf{r}_3, \mathbf{r}_4) = \langle \delta(\mathbf{r}_1)\delta(\mathbf{r}_2)\delta(\mathbf{r}_3)\delta(\mathbf{r}_4) \rangle$$

|||

$$\rho(\mathbf{r})/\bar{\rho} - 1 = n(\mathbf{r})/\bar{n} - 1$$

Overdensity

- Homogeneity: remove one coordinate

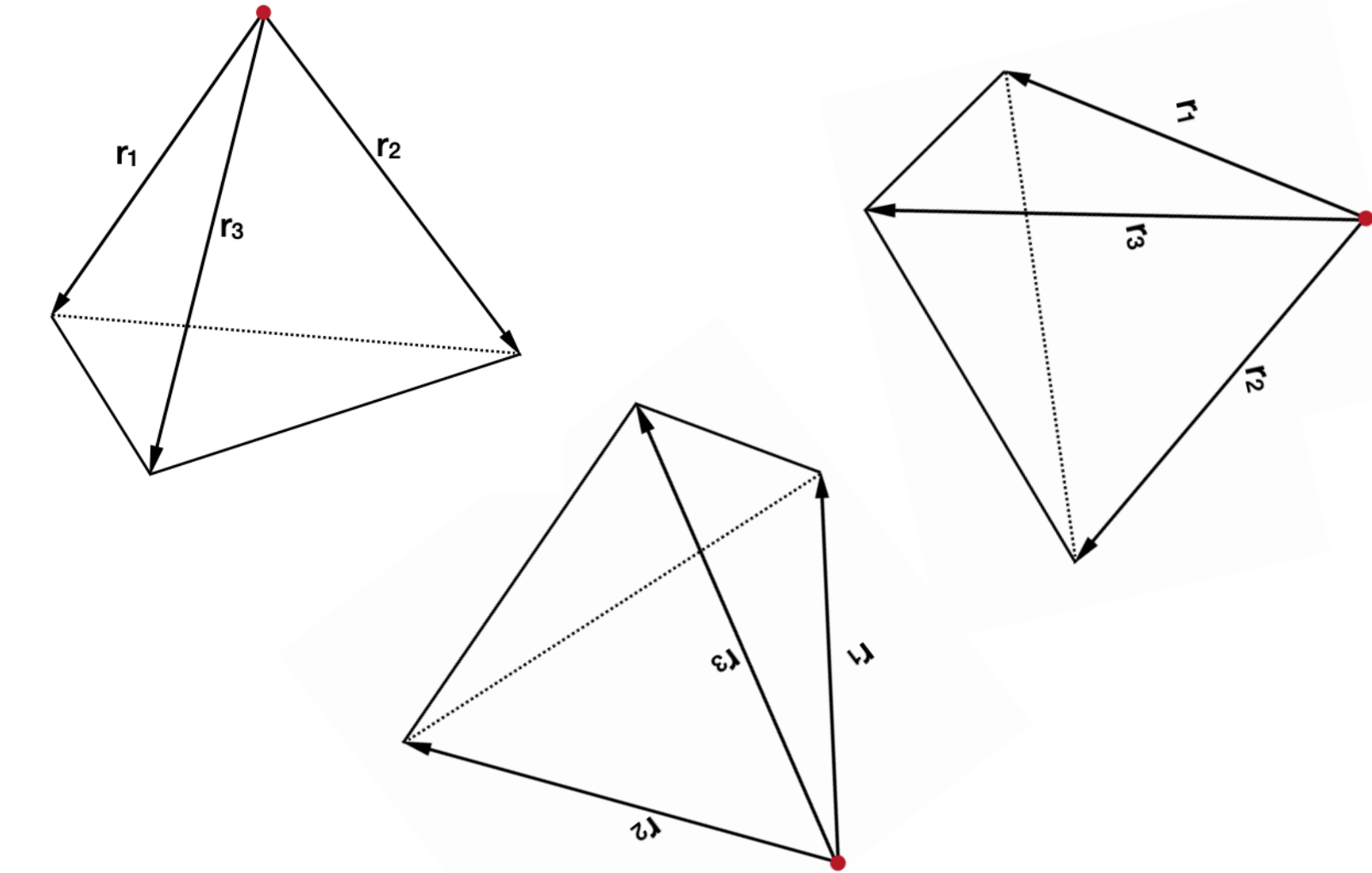
$$\zeta_g^4(\mathbf{r}_1, \mathbf{r}_2, \mathbf{r}_3, \mathbf{r}_4) \rightarrow \zeta_g^4(\mathbf{r}_1, \mathbf{r}_2, \mathbf{r}_3, \mathbf{r}_4 = 0)$$

Isotropy

- $\zeta_g^4(\hat{\mathbf{r}}_1, \hat{\mathbf{r}}_2, \hat{\mathbf{r}}_3)$ is a function of the relative orientations.
- Think about Legend polynomials.

$$P_\ell(\hat{\mathbf{r}}_1 \cdot \hat{\mathbf{r}}_2) = \frac{4\pi}{2\ell + 1} \sum_{m=-\ell}^{\ell} Y_{\ell_1}^m(\hat{\mathbf{r}}_1) Y_\ell^{*m}(\hat{\mathbf{r}}_2)$$

- The co-rotation invariant function are good basis functions and can be factorized into two spherical harmonics.



Isotropic basis functions

- How about three directions?

Cahn & Slepian '10

$$\mathcal{P}_{\ell_1, \ell_2, \ell_3}(\hat{\mathbf{r}}_1, \hat{\mathbf{r}}_2, \hat{\mathbf{r}}_3) \equiv \sum_{m_1, m_2, m_3} (-)^{\ell_1 + \ell_2 + \ell_3} \begin{pmatrix} \ell_1 & \ell_2 & \ell_3 \\ m_1 & m_2 & m_3 \end{pmatrix} Y_{\ell_1}^{m_1}(\hat{\mathbf{r}}_1) Y_{\ell_2}^{m_2}(\hat{\mathbf{r}}_2) Y_{\ell_3}^{m_3}(\hat{\mathbf{r}}_3)$$

3j symbol

The isotropic basis functions can be factorized into three spherical harmonics.

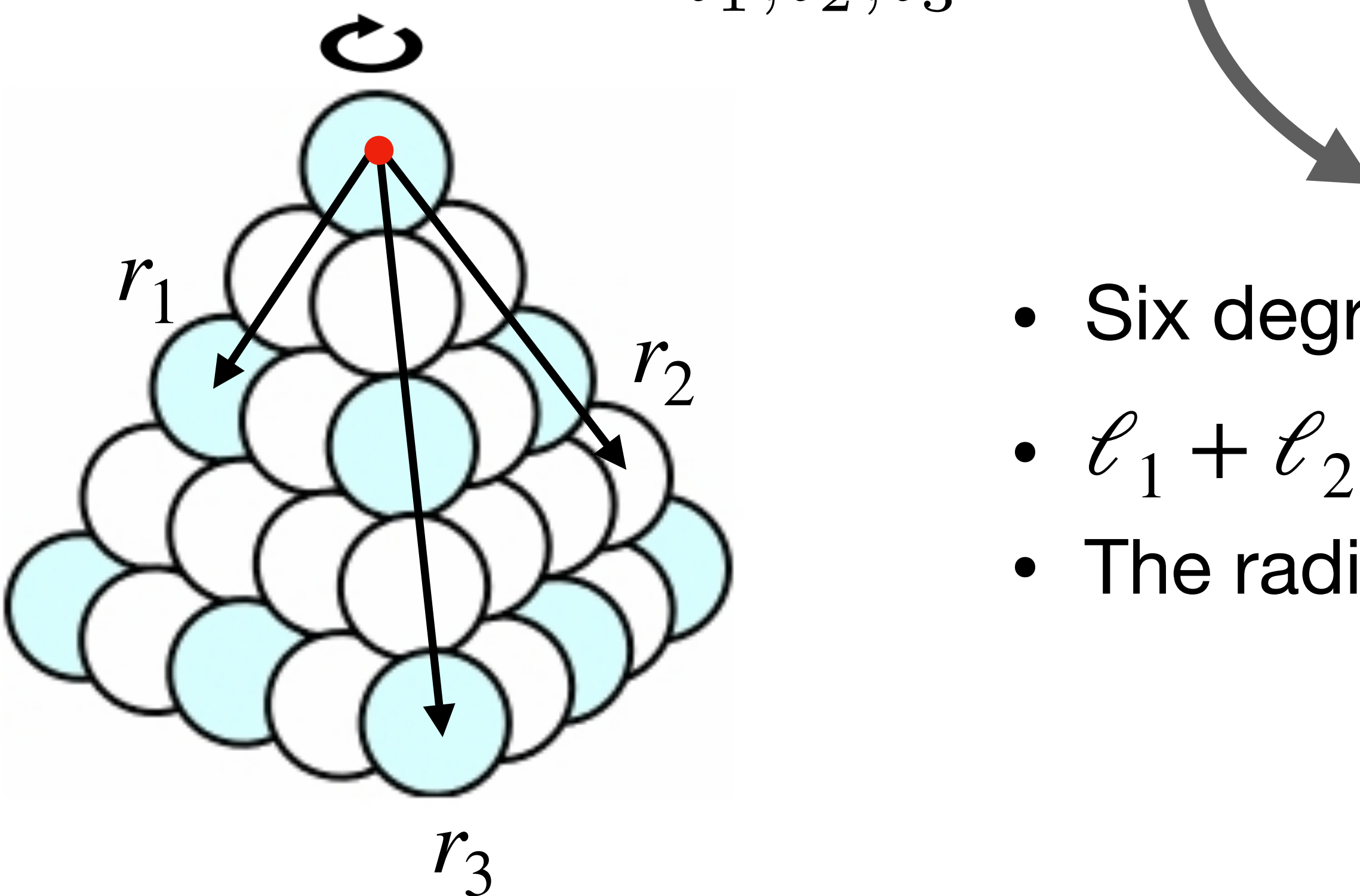
- Examples:

$$\mathcal{P}_{1,1,1}(\hat{\mathbf{r}}_1, \hat{\mathbf{r}}_2, \hat{\mathbf{r}}_3) \sim i \hat{\mathbf{r}}_1 \cdot (\hat{\mathbf{r}}_2 \times \hat{\mathbf{r}}_3)$$

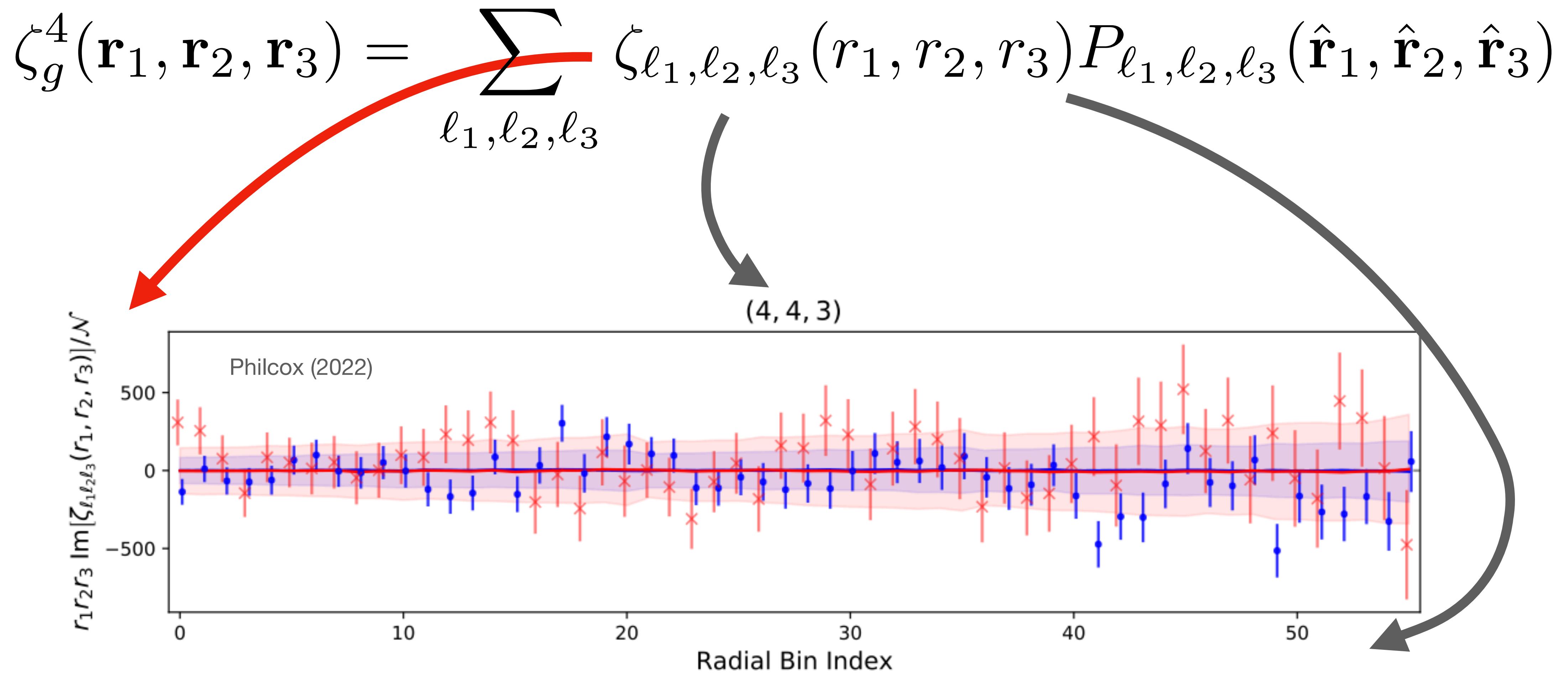
$$\mathcal{P}_{1,2,2}(\hat{\mathbf{r}}_1, \hat{\mathbf{r}}_2, \hat{\mathbf{r}}_3) \sim i \hat{\mathbf{r}}_1 \cdot (\hat{\mathbf{r}}_2 \times \hat{\mathbf{r}}_3)(\hat{\mathbf{r}}_2 \cdot \hat{\mathbf{r}}_3)$$

All the information is encoded in coefficients

$$\zeta_g^4(\mathbf{r}_1, \mathbf{r}_2, \mathbf{r}_3) = \sum_{\ell_1, \ell_2, \ell_3} \zeta_{\ell_1, \ell_2, \ell_3}(r_1, r_2, r_3) \mathcal{P}_{\ell_1, \ell_2, \ell_3}(\hat{\mathbf{r}}_1, \hat{\mathbf{r}}_2, \hat{\mathbf{r}}_3)$$



- Six degrees of freedom, $r_1, r_2, r_3, \ell_1, \ell_2, \ell_3$.
- $\ell_1 + \ell_2 + \ell_3 = \text{odd}$ means parity violating.
- The radii are discretized into radial bins.



Parity violating processes

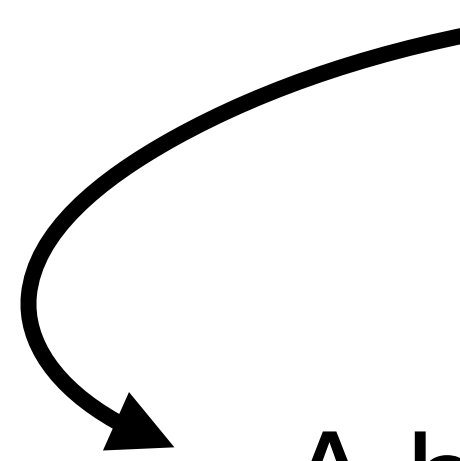
From trispectrum to 4PCF

$$\zeta(\mathbf{k}) \xrightarrow{\text{Boltzmann}} \delta(\mathbf{k}) \xrightarrow{\text{Galaxy bias}} \delta_g(\mathbf{k}) \xrightarrow{\text{Fourier trans.}} \delta_g(\mathbf{r})$$

Projection effect

$$\zeta_g^4(\mathbf{r}_1, \mathbf{r}_2, \mathbf{r}_3, \mathbf{r}_4) = \int \left[\prod_{i=1}^4 d^3 k_i Z_1(\hat{\mathbf{k}}_i, z) M(k_i, z) \right] \langle \zeta^4 \rangle'(\mathbf{k}) (2\pi)^3 \delta^3 \left(\sum_{i=1}^4 \mathbf{k}_i \right) \exp \left(\sum_{i=1}^4 i \mathbf{k}_i \cdot \mathbf{r}_i \right)$$

Kaiser redshift-space distortion Transfer function **Trispectrum** Momentum conservation Fourier kernel



A high-dim integral: N grids per dim $\Rightarrow N^{12}$ grids in total

From trispectrum to 4PCF

- **Factorizability** is the key in effectively performing the computation.
- A trispectrum needs to be factorized into **radial-angular** parts.

$$\mathbf{k}_s = \mathbf{k}_1 + \mathbf{k}_2$$

$$\langle \zeta_{\mathbf{k}_1} \zeta_{\mathbf{k}_2} \zeta_{\mathbf{k}_3} \zeta_{\mathbf{k}_4} \rangle' = \mathcal{J}(k_1, \dots, k_4, k_s) \mathcal{K}(\hat{\mathbf{k}}_1, \dots, \hat{\mathbf{k}}_4, \hat{\mathbf{k}}_s) + \text{perms}$$



Better to be further
separable.



Analytically integrated by
using Wigner symbols

Toy models

- Local shape * Parity-odd angular dependence

$$\langle \zeta^4 \rangle'_{\text{toy,local}} \propto P_\zeta(k_1)P_\zeta(k_2)P_\zeta(k_s)\mathcal{P}_{1,1,1}(\hat{\mathbf{k}}_1, \hat{\mathbf{k}}_3, \hat{\mathbf{k}}_s) + \text{perms}$$

curvature power spectrum

- Equilateral shape * Parity-odd angular dependence

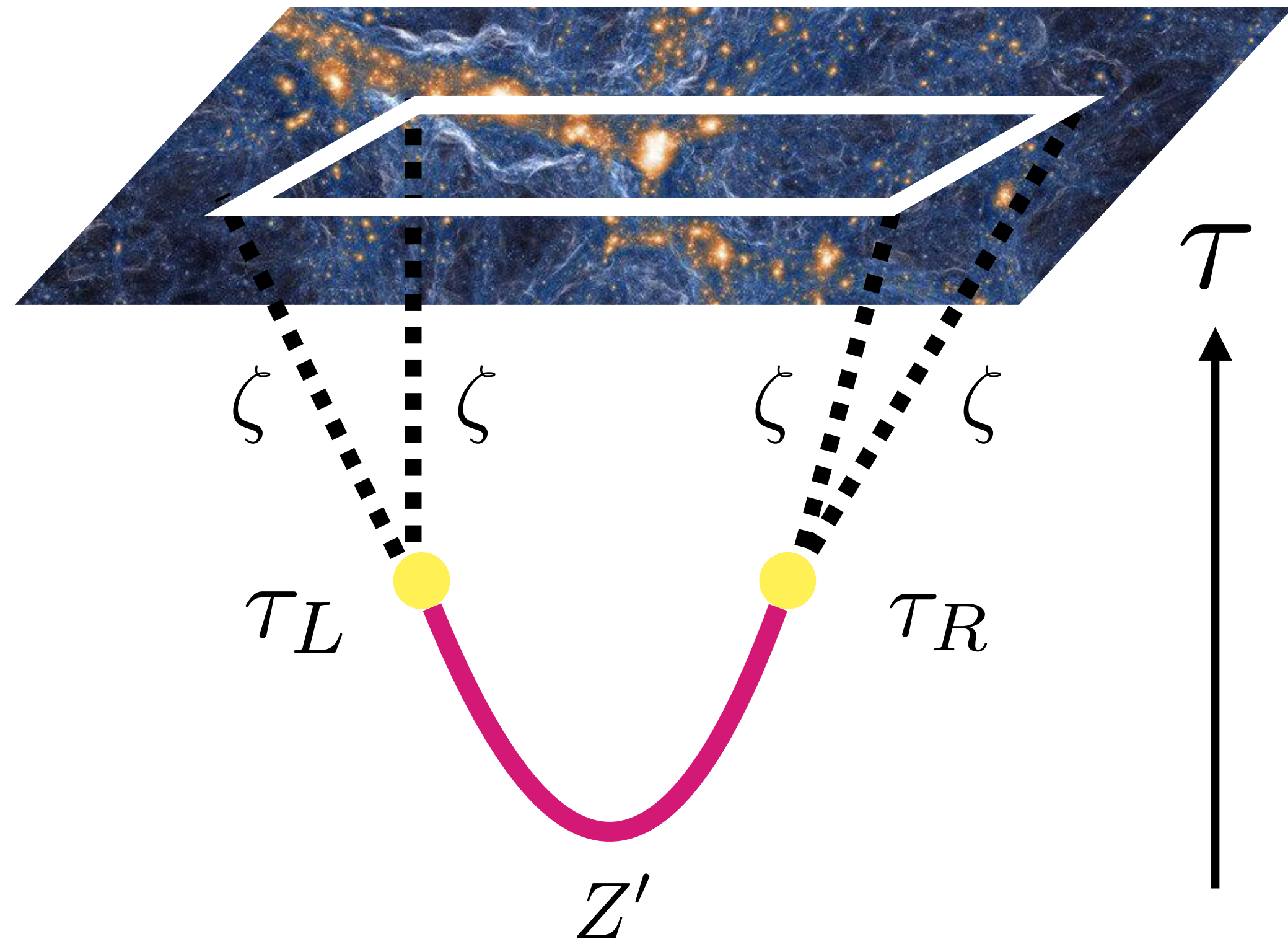
$$\langle \zeta^4 \rangle'_{\text{toy,eq}} \propto \frac{1}{k_1 k_2 k_3 k_4 k_t^5} \mathcal{P}_{1,1,1}(\hat{\mathbf{k}}_1, \hat{\mathbf{k}}_3, \hat{\mathbf{k}}_s) + \text{perms}$$

$k_t = \sum_{i=1}^4 k_i$ Factorizable by
Schwinger parametrization

Full model: massive spinning particle exchange

- Spin-1: Higgs model with gauge boson couples to a rolling background $\theta(t)$

$$\mathcal{L} = -\sqrt{-g} \left[\frac{1}{4} F_{\mu\nu} F^{\mu\nu} + D_\mu \Sigma^* D^\mu \Sigma - m_\Sigma^2 |\Sigma|^2 + \lambda |\Sigma|^4 \right] - \frac{c_0 \theta(t)}{4} \epsilon^{\mu\nu\rho\sigma} F_{\mu\nu} F_{\rho\sigma}$$

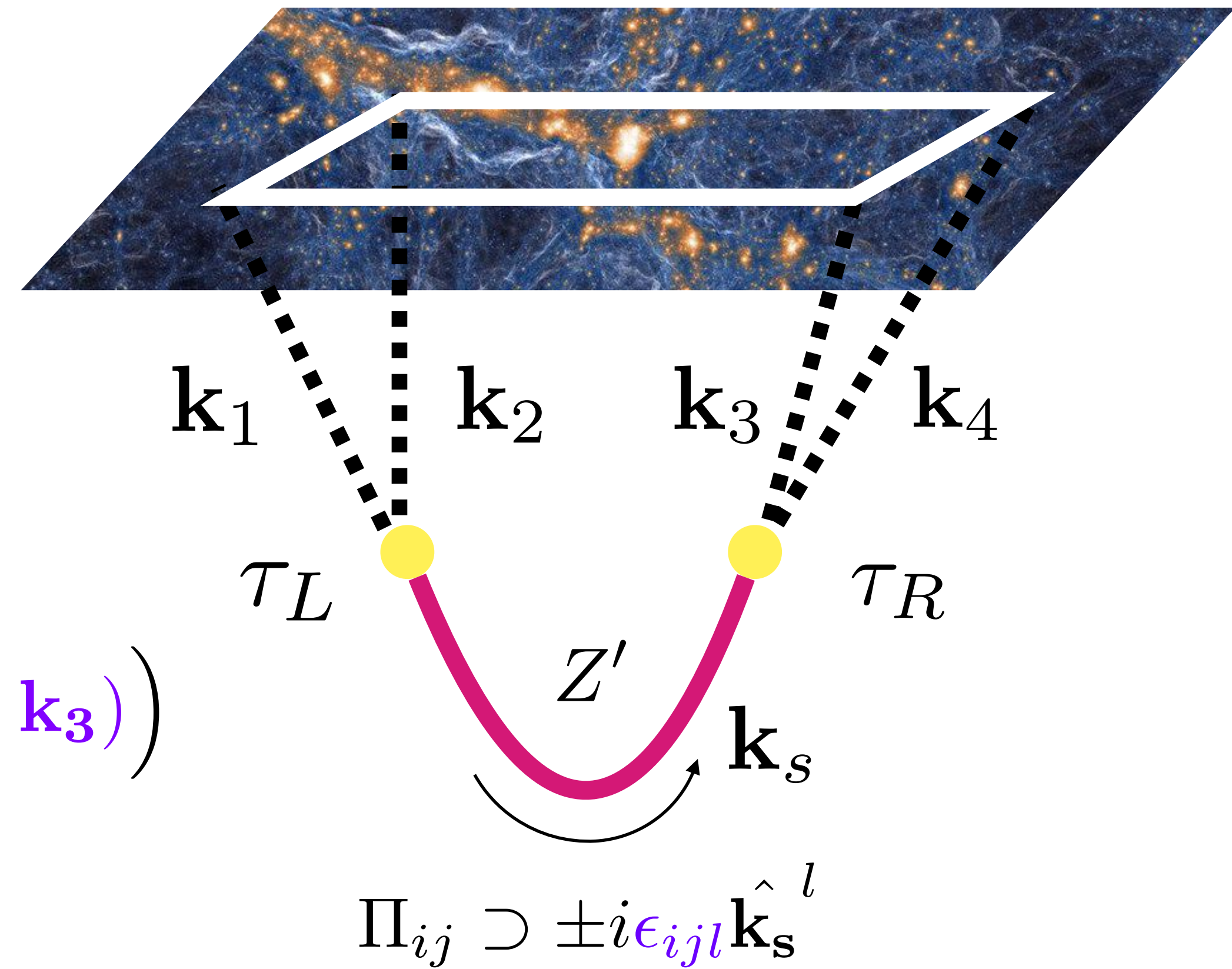


Liu, Tong, Wang, Xianyu '20, Wang & Xianyu '20

Full model: massive spinning particle exchange

- Advantage 1: signal is parity-violating.

$$\begin{aligned}\Pi &\propto (\mathbf{k}_1 \cdot \epsilon^{(-)}(\hat{\mathbf{k}}_s))(\mathbf{k}_3 \cdot \epsilon^{(-)}(\hat{\mathbf{k}}_s)) \\ &= \frac{1}{2} \left(\mathbf{k}_1 \cdot \mathbf{k}_3 - (\mathbf{k}_1 \cdot \hat{\mathbf{k}}_s)(\mathbf{k}_3 \cdot \hat{\mathbf{k}}_s) + i \hat{\mathbf{k}}_s \cdot (\mathbf{k}_1 \times \mathbf{k}_3) \right)\end{aligned}$$



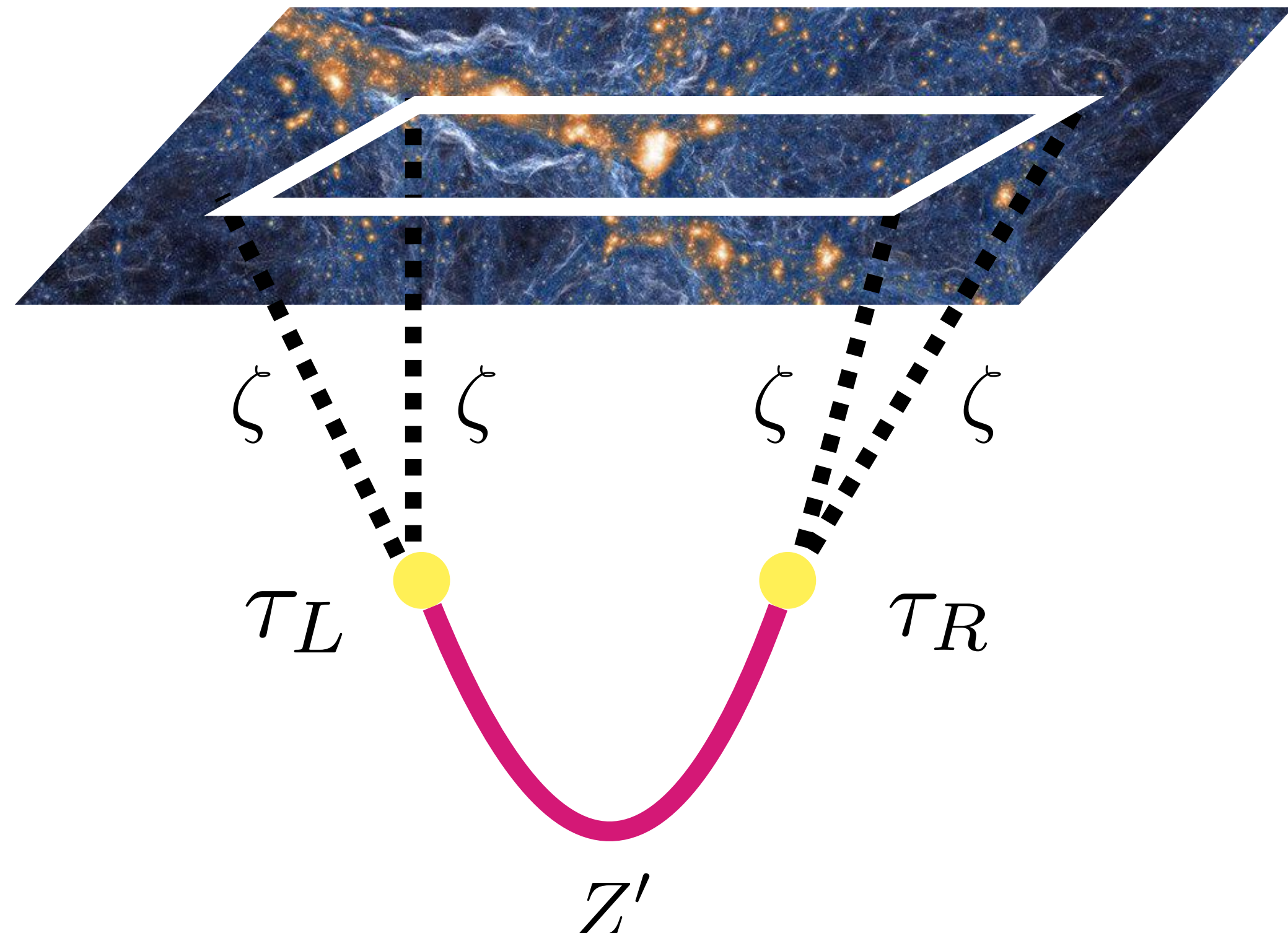
Full model: massive spinning particle exchange

- Advantage 2: signal could be sizable.

$c_0\theta(t)\epsilon^{\mu\nu\rho\sigma}F_{\mu\nu}F_{\rho\sigma}$ introduce a chemical potential of $\mu \equiv c_0\dot{\theta}$.

One of the transverse polarization will be enhanced and could overcome the Boltzmann suppression.

$$Z'_{(-)} : \langle \zeta^4 \rangle' \sim e^{-\pi m/H} \Rightarrow e^{\pi(\mu-m)/H}$$



Full model: massive spinning particle exchange

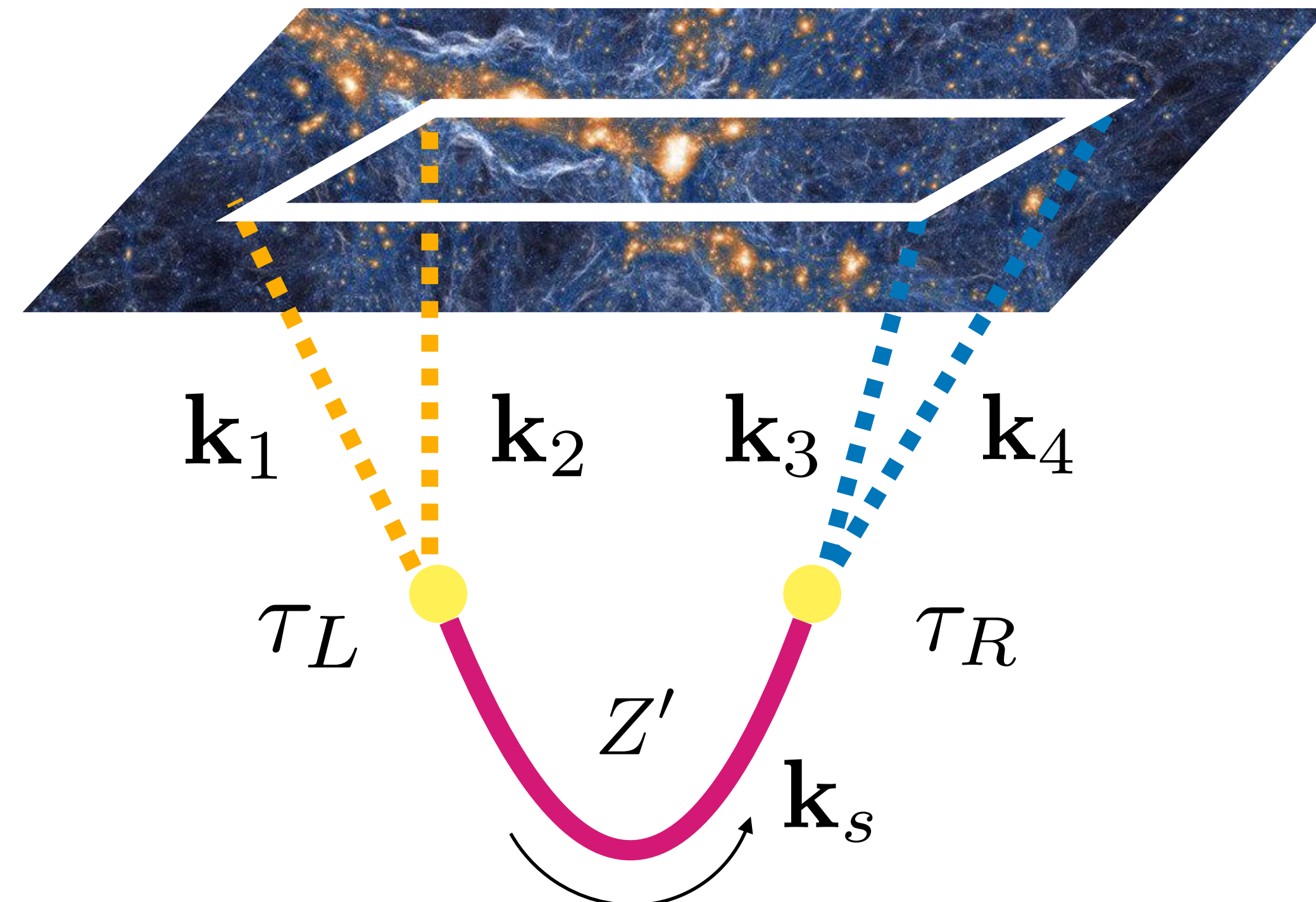
- Advantage 3: computation is factorizable.

The process can be expressed in tree-level SK diagrams

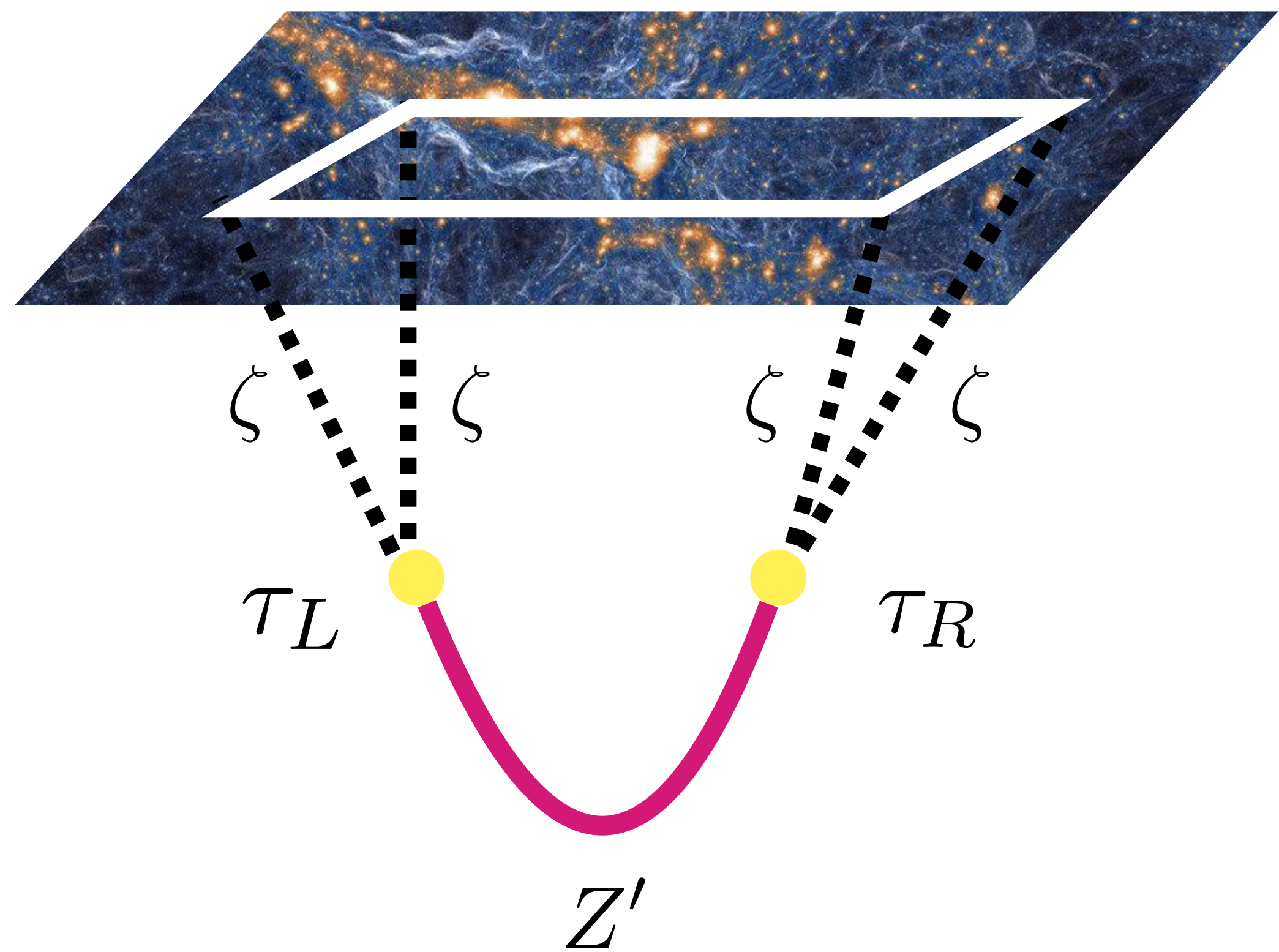


Naturally factorizable

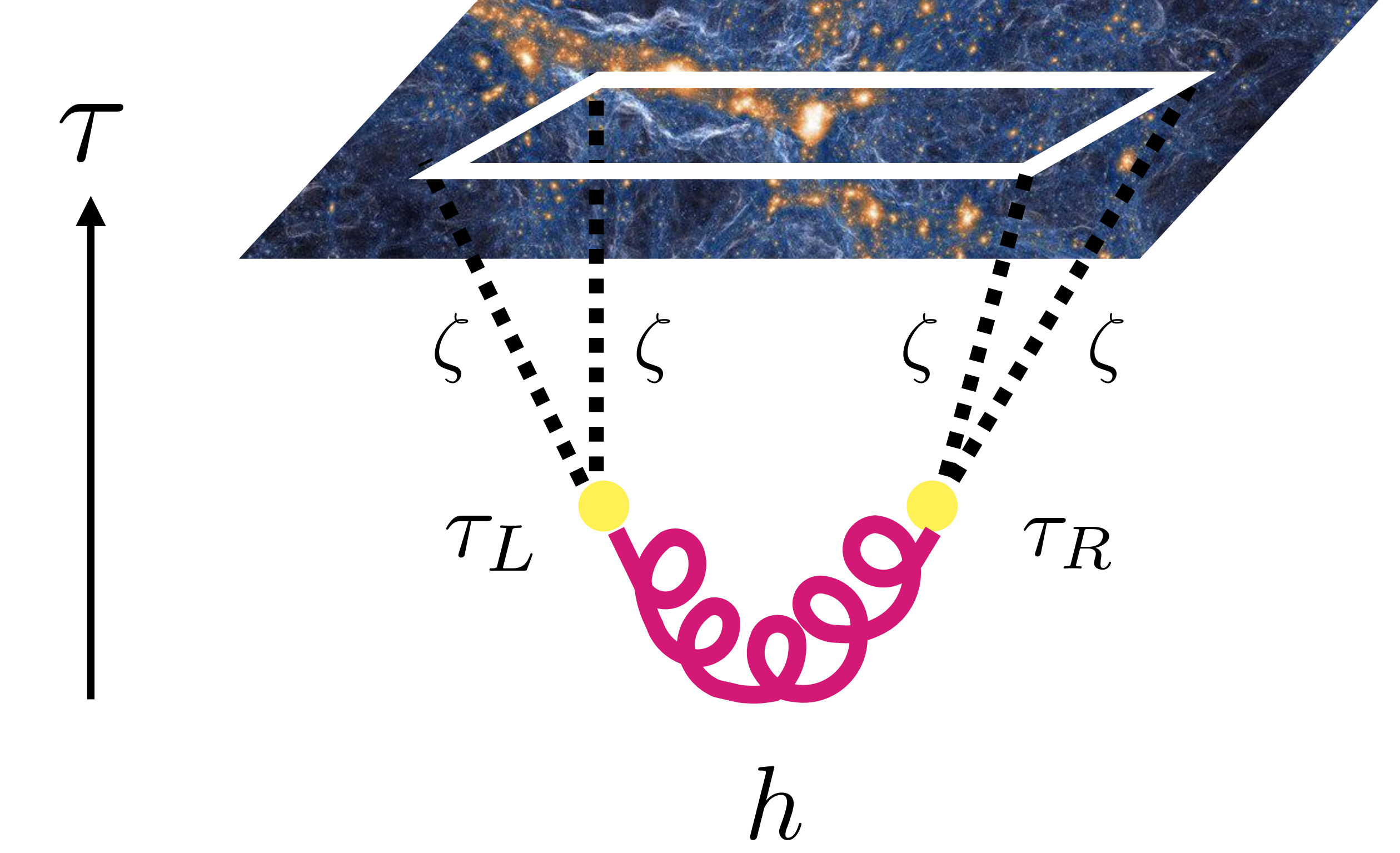
$$\langle \zeta^4 \rangle' \sim \int d\tau_L d\tau_R \mathcal{J}_L(k_1, k_2, k_s, \tau_L) \Pi(k_s, \tau_L, \tau_R) \mathcal{J}_R(k_3, k_4, k_s, \tau_R)$$



Full model: massive spinning particle exchange



Liu, Tong, Wang, Xianyu '20, Wang & Xianyu '20



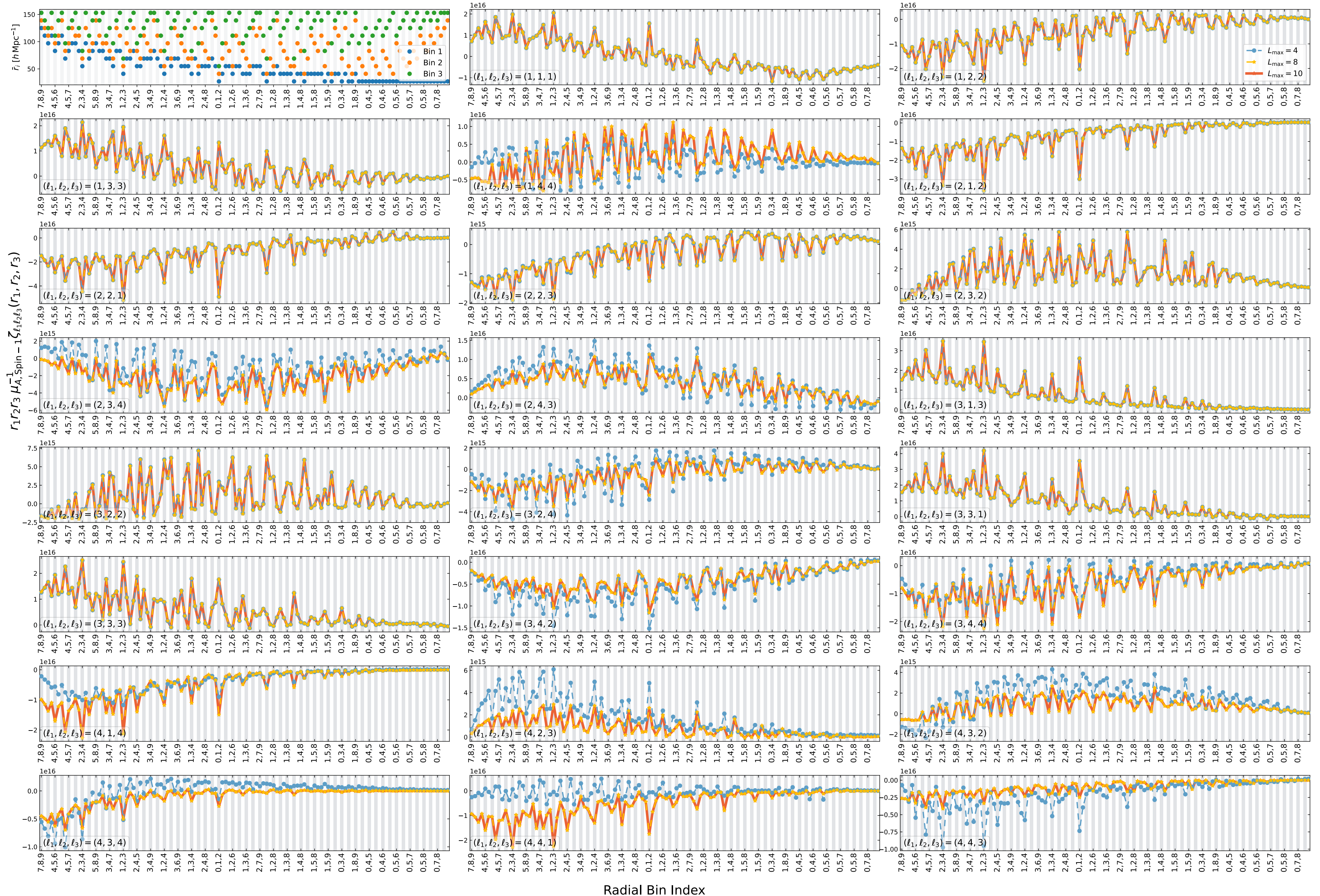
Tong & Xianyu '22

Result

General result

- 49 models in total

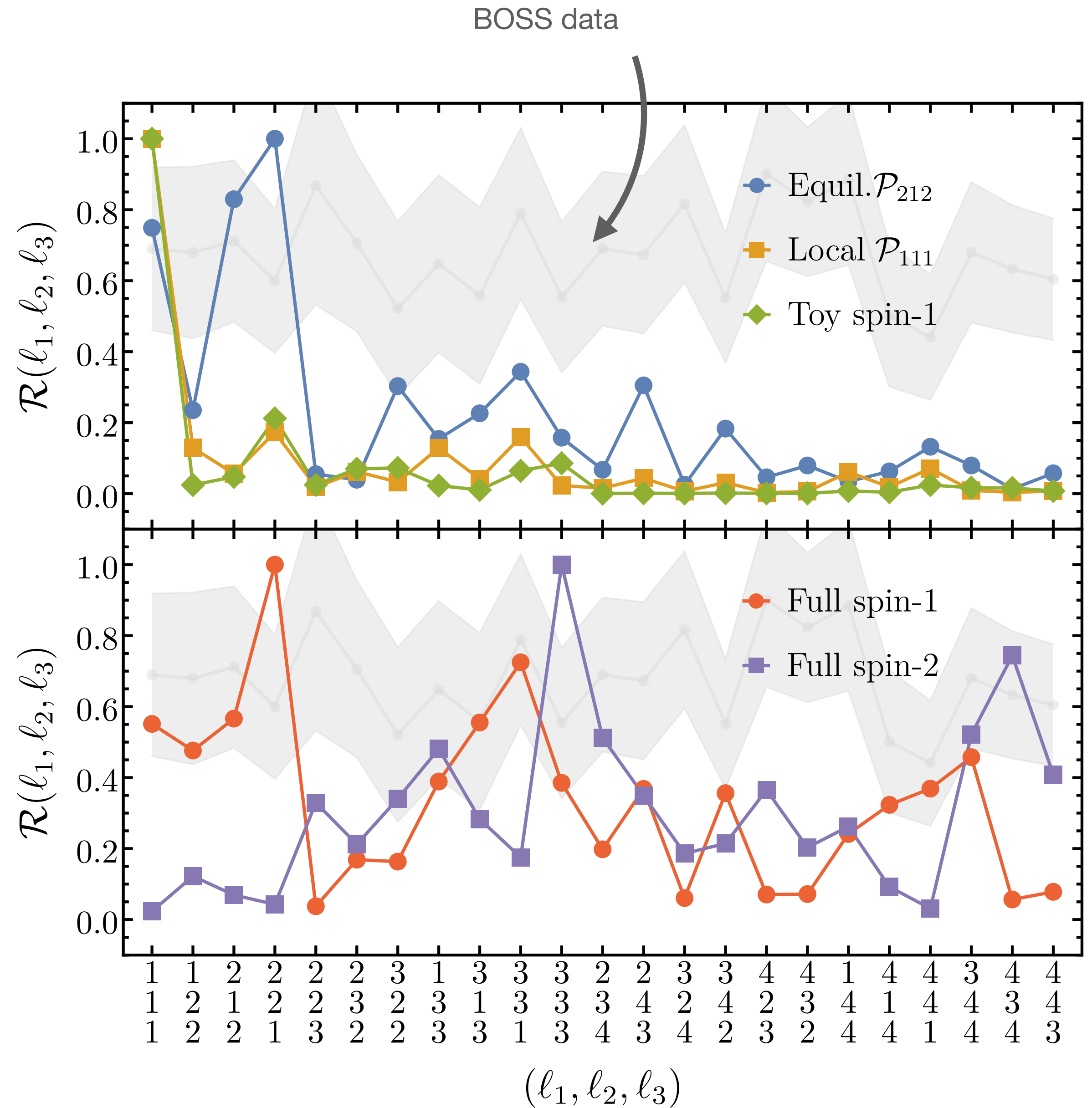
L_{\max} Dependence in Spin-1 model with $\tilde{v}_Z = c = 4$



Features: Angular part

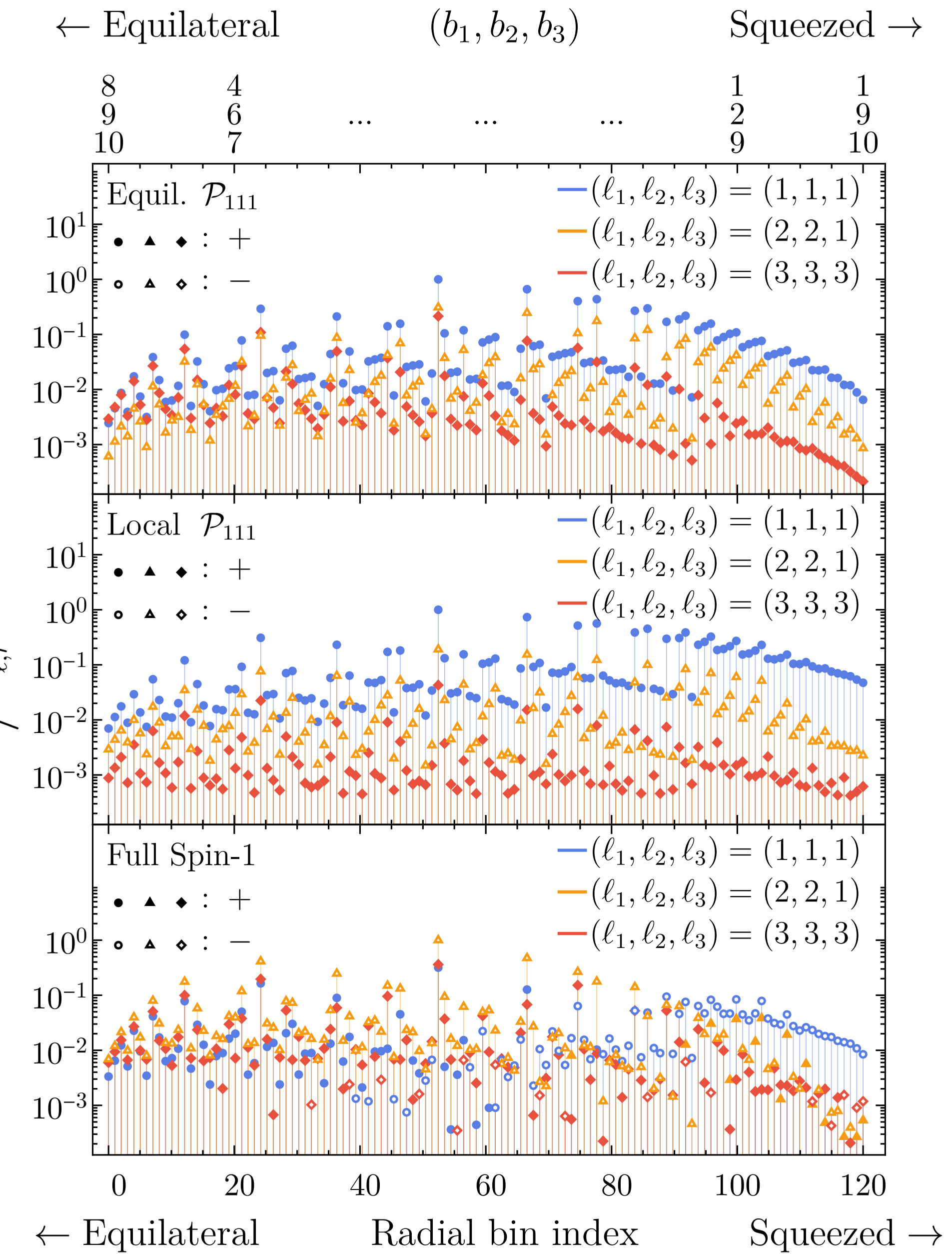
Coefficients marginalized over radii bins

- Trispectra with high- ℓ angular-dependence \Rightarrow Larger galaxy 4PCF signals in high- ℓ bins.
- Propagating degree carries spatial angular momentum \Rightarrow Signals spread over a large range of ℓ bins.



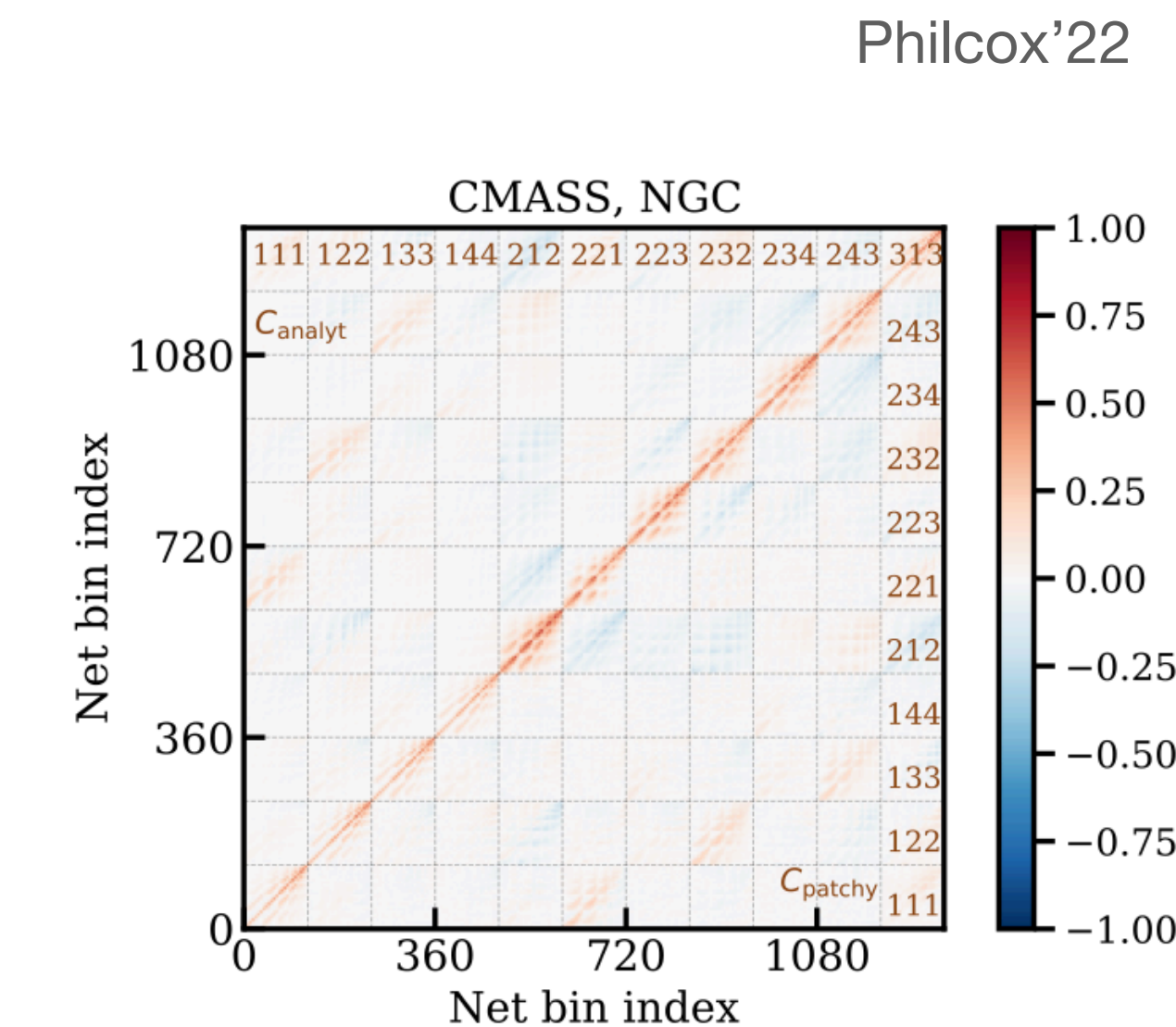
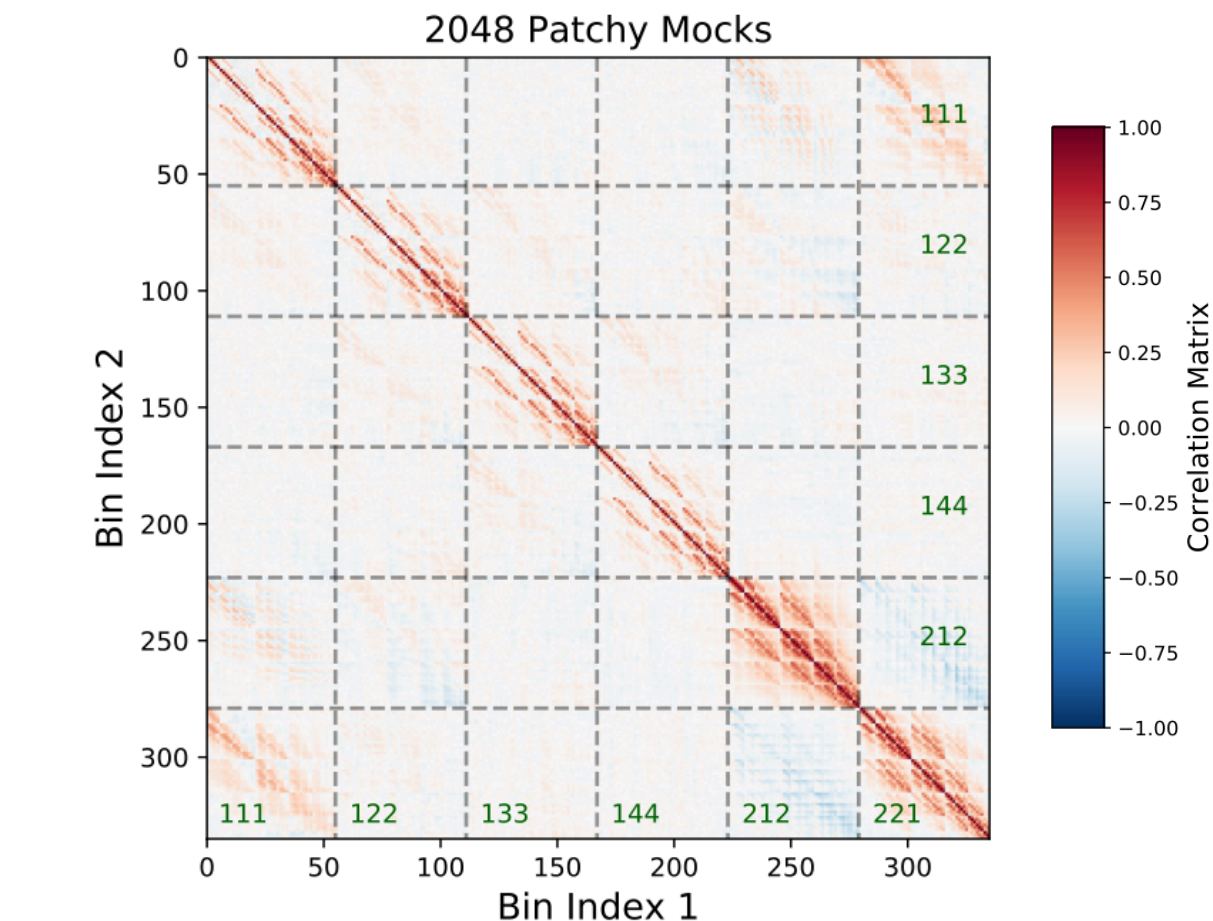
Features: Radial part

- The massive spinning exchange model shows more sign flips of the coefficients than the toy models.
 - The coefficients got suppressed for higher- ℓ bins. For Equil. Model and full spin-1 model, the suppression mostly happens at the squeezed limit.



Comparison w/ BOSS

- Philcox (2022) and Hou, Slepian & Cahn (2022) both used the compressed χ^2 analysis pipeline and covariance matrix from the same set of simulations.
- Looking for the most robust linear combination of basis functions \Rightarrow **keeping N_{eig} eigenvectors with smallest eigenvalues of the covariance matrix.**
- Remove small-scale effects \Rightarrow **filtering out near-by radii bin combos.**

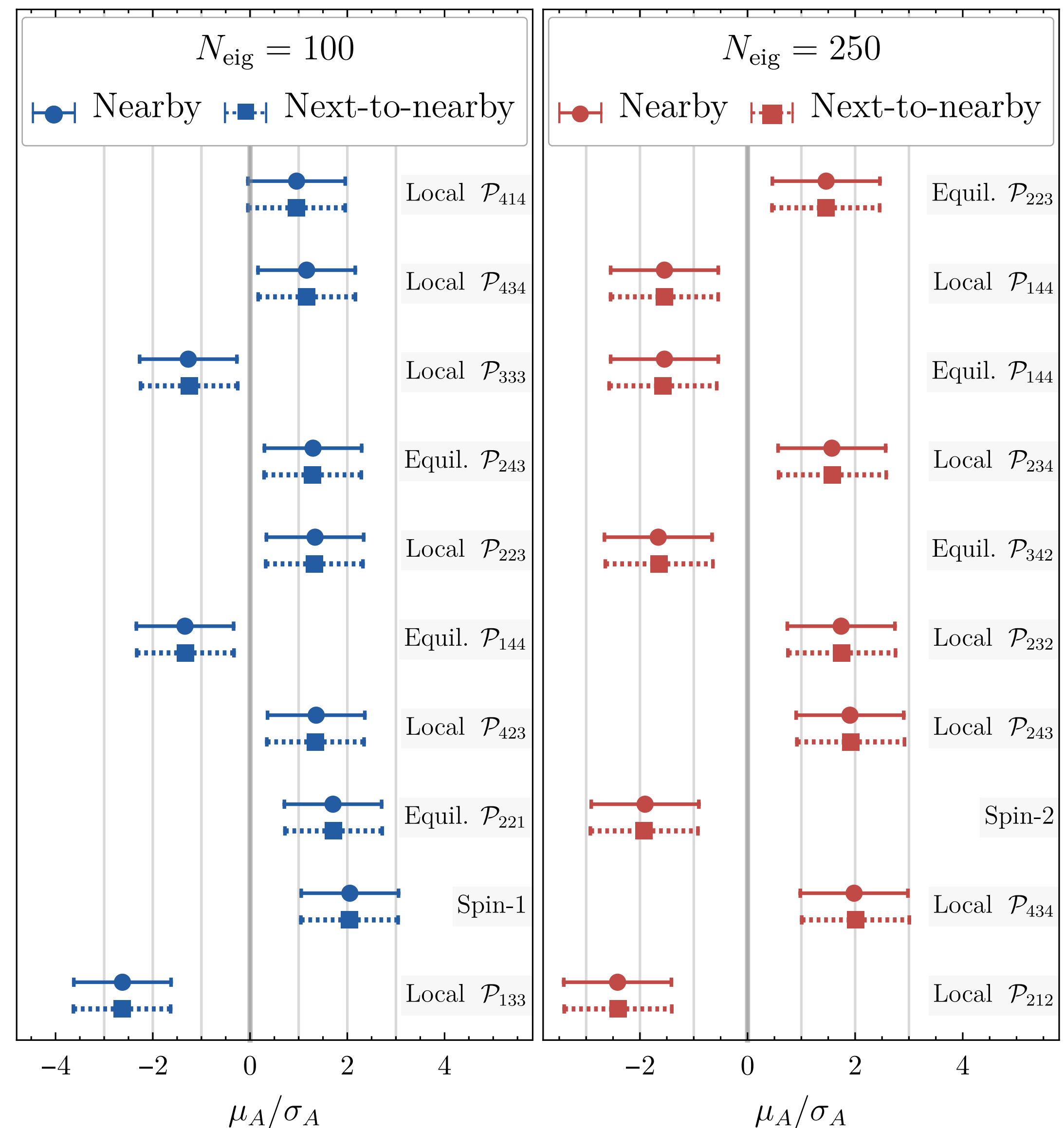


Hou, Slepian & Cahn '22

Comparison w/ BOSS

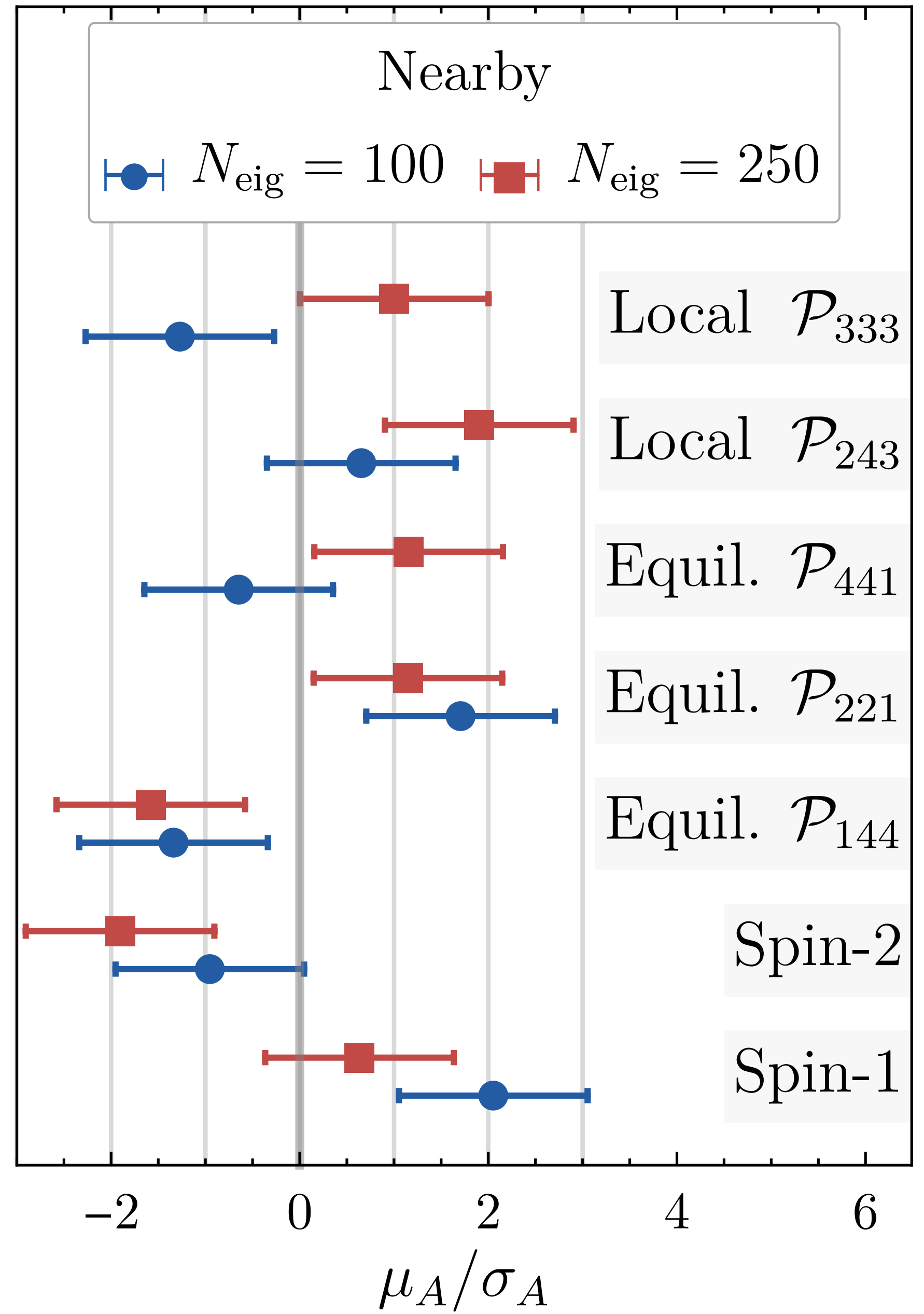
- Top 10 models with highest scaling factor over its standard deviation μ_A/σ_A .
- No models passing detection level of 3σ .
- The radial bin filtering has negligible effects.

For spin-1 and 2 models, $\mu \equiv \sqrt{m^2/H^2 - 9/4} = 4$
 Chemical potential enhancement $e^{4\pi}$



Comparison w/ BOSS

- μ_A/σ_A fluctuates for the same model with different N_{eig} .
- Questions into the robustness of compressed χ^2 methods.
- Useful information of the parity-violation is likely dropped out due to data compression.



Summary

- Parity violation in correlation functions represents novel opportunities in detecting PNGs.
- High dimensionality poses a significant challenge in converting parity-violating trispectra into galaxy 4PCF. Factorization is necessary.
- Massive spinning particle exchange with chemical-potential enhancement is a type of well-suited models for parity violation detection.